

GRB 070610: A CURIOUS GALACTIC TRANSIENT

M. M. KASLIWAL¹, S. B. CENKO², S. R. KULKARNI¹, P. B. CAMERON¹, E. NAKAR¹, E. O. OFEK¹, A. RAU¹, A. M. SODERBERG¹, S. CAMPANA³, J. S. BLOOM⁴, D. A. PERLEY⁴, L. POLLACK⁴, S. BARTHELMY⁵, J. CUMMINGS⁵, N. GEHRELS⁵, H. A. KRIMM^{6,16}, C. B. MARKWARDT^{6,7}, G. SATO⁵, P. CHANDRA⁸, D. FRAIL⁹, D. B. FOX¹⁰, P. PRICE¹¹, E. BERGER^{12,13}, S. A. GREBENEV¹⁴, R. A. KRIVONOS^{14,15} & R. A. SUNYAEV^{14,15}

October 26, 2018

ABSTRACT

GRB 070610 is a typical high-energy event with a duration of 5 s. Yet within the burst localization we detect a highly unusual X-ray and optical transient, *Swift* J195509.6+261406. We see high amplitude X-ray and optical variability on very short time scales even at late times. Using near-infrared imaging assisted by a laser guide star and adaptive optics, we have identified a quiescent counterpart to *Swift* J195509.6+261406. Our spectroscopic observations show that the spectral type of the counterpart is likely a K dwarf/sub-giant. It is possible that GRB 070610 and *Swift* J195509.6+261406 are unrelated sources. However, the absence of a typical X-ray afterglow from GRB 070610 in conjunction with the spatial and temporal coincidence of GRB 070610 and *Swift* J195509.6+261406 motivate us to suggest that the sources are related. The closest analog to *Swift* J195509.6+261406 is V4641 Sgr, an unusual black hole binary. We suggest that GRB 070610 along with V4641 Sgr define a sub-class of stellar black holes – the fast X-ray novae. We further suggest that fast X-ray novae are associated with bursts of gamma-rays. If so, GRB 070610/*Swift* J195509.6+261406 defines a new class of gamma-ray bursts and these bursts dominate the long-duration GRB demographics.

Subject headings: gamma rays:bursts – X-rays:bursts – X-rays: individual (Swift J195509.6+261406) – stars:flare – X-rays: binaries

1. DISCOVERY OF GRB 070610

Launched in November 2004, the *Swift* Gamma-Ray Burst Explorer (Gehrels et al. 2004) was designed to localize γ -ray bursts (GRBs) and undertake rapid and sustained X-ray and Ultra-Violet observations of the resulting afterglow. With over two hundred events now localized and studied, *Swift* has made fundamental contributions to both long-duration soft bursts (LSBs) and

short-duration hard bursts (SHBs). LSBs appear to trace cosmological massive-star formation rate with one event at a redshift of 6.4. SHBs have been seen at typical redshifts of ~ 0.5 in both elliptical and star-forming galaxies. There is now some circumstantial evidence for SHBs being the result of coalescence of compact objects.

At 20:52:26 UT on 2007 June 10 the Burst Alert Telescope (BAT; Barthelmy et al. 2005) aboard *Swift* triggered on GRB 070610. The high-energy prompt emission had a duration (T_{90}) of 4.6 s (Paganini et al. 2007a). Over the range 15–150 keV the burst could be fitted with a power law with photon index $\Gamma = 1.76 \pm 0.25$, resulting in a fluence of $(2.4 \pm 0.4) \times 10^{-7}$ erg cm⁻² (Tueller et al. 2007). A blackbody model is inconsistent with this emission.

The burst profile consisted of a single symmetric peak (Figure 1). Fitting the profile (Norris et al. 1996), we calculate a rise time (i.e. half width at half maximum) of 1.68 ± 0.55 s. As can be seen from Figure 2, the duration and the hardness ratio of *Swift* J195509.6+261406 are both consistent with the broader population of extragalactic long-duration GRBs observed by *Swift*.

The BAT localized GRB 070610 to $\alpha = 19^{\text{h}}55^{\text{m}}13\overset{\text{s}}{.}1$, $\delta = +26^{\circ}15'20''$ (J2000.0) and a 90%-containment radius of $1.8'$. As can be seen in Figure 3 the field is dense, which is not surprising given the Galactic location ($l = 63.3^{\circ}$ and $b = -1.0^{\circ}$).

Here we report the discovery of an unusual X-ray transient (hereafter referred to as *Swift* J195509.6+261406) in the error circle of GRB 070610 and followup optical, near-infrared (NIR) and radio observations.

2. *Swift* J195509.6+261406: A TRANSIENT X-RAY SOURCE

¹ Division of Physics, Mathematics and Astronomy, California Institute of Technology, MS 105-24, Pasadena, CA 91125, USA

² Space Radiation Laboratory, California Institute of Technology, MS 220-47, Pasadena, CA 91125, USA

³ INAF, Osservatorio Astronomico di Brera, via E. Bianchi 46, I-23807 Merate (LC), Italy

⁴ Department of Astronomy, University of California, Berkeley, CA 94720, USA

⁵ NASA Goddard Space Flight Center, Greenbelt, MD 20771, USA

⁶ CRESST and Astroparticle Physics Laboratory, NASA/GSFC, Greenbelt, MD 20771, USA

⁷ Department of Astronomy, University of Maryland, College Park, MD 20742, USA

⁸ University of Virginia, P.O. Box 400325, Charlottesville, VA 22903, USA

⁹ National Radio Astronomy Observatory, Socorro, NM 87801, USA

¹⁰ Department of Astronomy & Astrophysics, 525 Davey Laboratory, Pennsylvania State University, University Park, PA 16802, USA

¹¹ Institute for Astronomy, University of Hawaii, 2680 Woodlawn Drive, Honolulu, HI 96822, USA

¹² Observatories of the Carnegie Institute of Washington, Pasadena, CA 91101, USA

¹³ Princeton University Observatory, Princeton, NJ 08544, USA

¹⁴ Space Research Institute, Profsoyuznaya 84/32, 117997 Moscow, Russia

¹⁵ Max-Plank-Institut fuer Astrophysik, Karl-Schwarzschild-Str. 1, D-85741 Garching, Germany

¹⁶ Universities Space Research Association, 10211 Winthrop Circle, Suite 500, Columbia, MD 21044

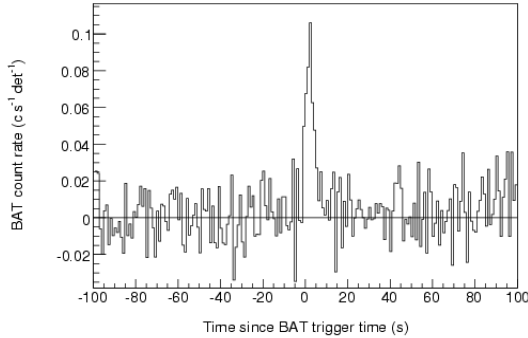


FIG. 1.— 15–150 keV *Swift*-BAT light curve of GRB 070610, with 1-s time resolution. The conversion factor to translate the ordinate to cgs flux units is 5.6×10^{-7} erg cm $^{-2}$ c $^{-1}$ det (1 det = 0.16 cm 2).

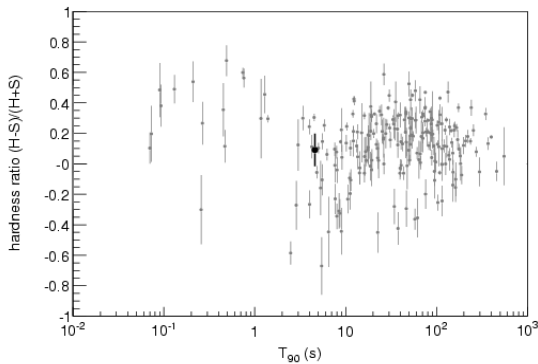


FIG. 2.— Plot of duration (T_{90}) and hardness ratio (HR) of 226 *Swift* bursts from GRB 041217 to GRB 070616. We define hardness ratio as $(H - S)/(H + S)$, where S and H are energy fluences in 15–50 keV and 50–150 keV, respectively. The values of T_{90} and hardness ratio for GRB 070610 (marked by a large filled black circle) are 4.6 ± 0.4 s and 0.09 ± 0.11 (90% confidence level), respectively.

The X-ray Telescope (XRT; Burrows et al. 2005) began observing the field of GRB 070610 3.2 ks after the initial BAT trigger (prompt slewing was disabled due to an Earth limb constraint). The XRT detected a single uncatalogued variable source in the BAT error circle at $\alpha = 19^{\text{h}}55^{\text{m}}9\overset{\text{s}}{.}6$, $\delta = +26^{\circ}14'6\overset{\text{s}}{.}7$ (90% confidence error circle of $4\overset{\prime}{.}3$ radius; Pagani et al. 2007b). This position was further refined to $\alpha = 19^{\text{h}}55^{\text{m}}9\overset{\text{s}}{.}66$, $\delta = +26^{\circ}14'5\overset{\text{s}}{.}2$ (90% confidence error circle of $1\overset{\prime}{.}2$ radius¹⁷).

The XRT continued to monitor *Swift* J195509.6+261406 over the course of the next month until the source was no longer detected.

The XRT data were processed with standard procedures (`xrtpipeline v0.10.6`). All data were obtained in photon counting mode. In this mode the entire CCD is read and the time resolution is limited to 2.5 s. We extracted grade 0–12 events (Burrows et al. 2005) from a 15 pixel radius circular region centered on the source. To account for the background, we extracted events within

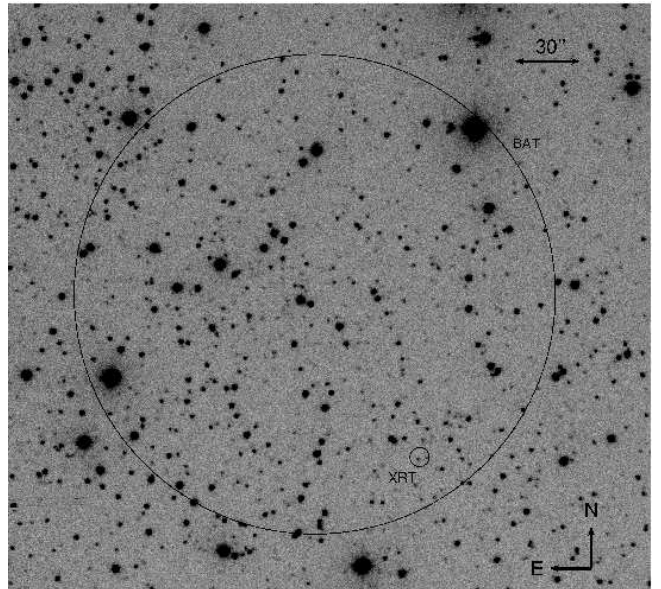


FIG. 3.— Optical image (i' -band) of the field of GRB 070610 obtained by the automated Palomar 60-inch telescope on 2007 June 12. The BAT localization of GRB 070610 has a radius of $1.8'$, while the XRT localization of *Swift* J195509.6+261406 has a radius of $4.3''$; both are indicated with black circles. The bright source in the XRT circle is *Swift* J195509.6+261406 .

a 40 pixel radius circular region in the vicinity of the transient but not encompassing any other source in the field. We adaptively extracted the light curve binning the data in order to have 10 counts per bin. The light curve was corrected for the extraction region losses and for CCD defects as well as for vignetting by using the task `xrtlccorr` (v0.1.9), which generates an orbit-by-orbit correction based on the instrument map.

The X-ray light curve of *Swift* J195509.6+261406 is shown in Figure 4 and compared to a small sample of long-duration GRB afterglows in Figure 5. Clearly, *Swift* J195509.6+261406 differs from typical GRB X-ray light curves in two fundamental respects. First, it does not exhibit the strong (overall) secular decrease in flux, over timescales of hours, seen in afterglows of GRBs (Nousek et al. 2006; Zhang et al. 2006). While the decay index in long-duration GRBs can vary markedly from one phase to another, *Swift* J195509.6+261406 shows no significant decline until very late times ($\sim 10^6$ s).

Secondly, the XRT light curve of *Swift* J195509.6+261406 consists of spikes – never seen before in any afterglow. In particular we draw the attention of the reader to a dramatic flare at $t \sim 7.86 \times 10^4$ s, jumping by a factor of $\Delta f/f \sim 100$ in flux over a time scale of $\Delta t/t \sim 10^{-4}$ (see Figure 4, inset). None of the 69 XRT flares described in Chincarini et al. (2007) exhibit a comparable amplitude spike at late time. While a strong X-ray flare has been seen in GRB 050502B (Falcone et al. 2006) (see Figure 5) the fractional duration, $\Delta t/t$ is much larger (~ 0.5). Less significant variability is present throughout the duration of observations of *Swift* J195509.6+261406 .

We searched the XRT flare for pulsations. 521 photons were extracted within $60''$ of the source position and corrected to the solar system barycenter with the task

¹⁷ http://astro.berkeley.edu/~nat/swift/xrt_pos.html

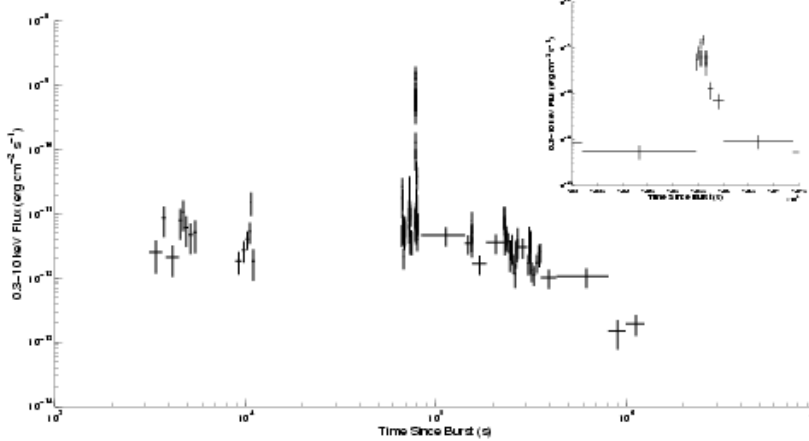


FIG. 4.— XRT light curve of *Swift* J195509.6+261406 in the energy band 0.3–10 keV. One count s^{-1} corresponds to about $1.3 \times 10^{-10} \text{ erg cm}^{-2} \text{ s}^{-1}$. The dramatic X-ray flare at $t \sim 7.86 \times 10^4 \text{ s}$ is shown in the inset.

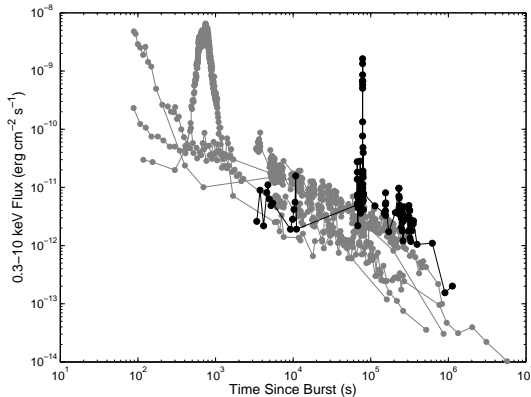


FIG. 5.— XRT Light curves of a small sample of extra-galactic long-duration GRBs (GRBs 050315, 050318, 050319, 050416A, and 050502B) are shown in grey. Data are from Evans et al. 2007. All show the approximately power-law decay typical of GRB afterglows. GRB 050502B exhibits a bright flare around $t \sim 10^3 \text{ s}$ (see Falcone et al. 2006). However, the rise time of this flare is much longer than the spike seen in *Swift* J195509.6+261406 (shown in black).

barycorr. To search for pulsations we constructed the Z_1^2 power spectrum to a maximum frequency of 0.2 Hz (Buccheri et al. 1983). The largest observed value of Z_1^2 was 25.2 at a frequency of 0.1446 Hz. Since Z_n^2 is distributed as χ^2 with $2n$ degrees of freedom, this value corresponds to a single trial detection significance of 4.8σ in equivalent Gaussian units. Given that we have performed 350 trials, the significance of this detection is 3.4σ , and thus we do not consider this result to be conclusive evidence of periodicity.

For spectral analysis the ancillary response files were generated with the task `xrtmkarf`. We used the latest spectral redistribution matrices (v009). Data were extracted from single or consecutive orbits in order to have at least 100 counts per spectrum. Spectra were binned to a minimum of 15 counts per energy bin. The resulting four spectra were inconsistent with a blackbody and consistent with a power law model (task `pabs`). The

TABLE 1
XRT SPECTRAL ANALYSIS

Epoch Start (MJD)	Total Exposure (s)	N_{H} (10^{22} cm^{-2})	Γ
54261.907	4811	$0.30^{+0.29}_{-0.23}$	1.43 ± 0.37
54262.641	7912	$0.76^{+0.24}_{-0.18}$	1.93 ± 0.18
54263.268, 54264.004	2947, 10500	$0.59^{+0.31}_{-0.23}$	1.11 ± 0.22
54265.387	6026	$0.61^{+0.53}_{-0.33}$	1.33 ± 0.40
Flare	...	$0.92^{+0.91}_{-0.57}$	1.74 ± 0.48
All but flare	...	$0.72^{+0.14}_{-0.12}$	1.71 ± 0.11

NOTE. — We have fit the XRT data to a power-law model of the form $N(E) \propto E^{-\Gamma}$, leaving the line-of-sight N_{H} as a free parameter.

best fit column density (N_{H}) and photon index (Γ) for each epoch are summarized in Table 1. Overall, we find that the inferred flux conversion is approximately 1 count $\text{s}^{-1} \approx 1.3 \times 10^{-10} \text{ erg cm}^{-2} \text{ s}^{-1}$ in the 0.3–10 keV band.

We extrapolate the XRT flare spectrum to BAT(15–50 keV) and predict a flux of $1.8 \times 10^{-9} \text{ erg cm}^{-2} \text{ s}^{-1}$. This corresponds to a BAT count rate of 0.0032 counts $\text{s}^{-1} \text{ det}^{-1}$. This is consistent with a 2σ upper limit from two 64s intervals of BAT data straddling the XRT flare — 0.0038 counts $\text{s}^{-1} \text{ det}^{-1}$ (at 78499.8 s) and 0.012 counts $\text{s}^{-1} \text{ det}^{-1}$ (at 78563.8 s).

The inferred interstellar extinction along this low Galactic latitude is quite high and thus uncertain: N_{H} of $1.1 \times 10^{22} \text{ cm}^{-2}$ (Dickey & Lockman 1990); $0.8 \times 10^{22} \text{ cm}^{-2}$ (Kalberla et al. 2005); and $1.56 \times 10^{22} \text{ cm}^{-2}$ (Schlegel et al. 1998). The former two estimates are based on H I data whereas the latter on diffuse infrared emission. Given the uncertainty in the inferred N_{H} the XRT spectrum cannot be used to constrain the distance to *Swift* J195509.6+261406.

3. A FLICKERING OPTICAL VARIABLE

Rapid observations in response to the BAT trigger, in particular by the *OPTIMA-Burst* team (Stefanescu et al. 2007b), revealed a rapidly variable (time scales as low as tens of seconds) optical transient inside the XRT error circle of *Swift* J195509.6+261406.

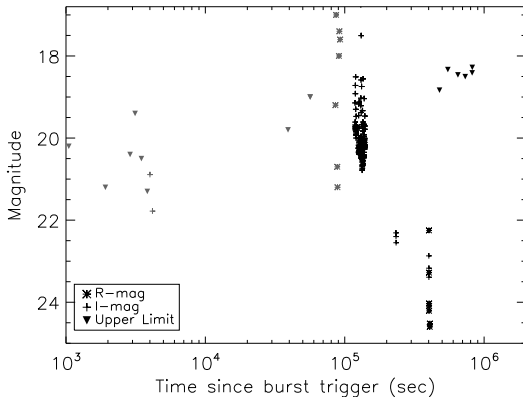


FIG. 6.— Optical light curve of *Swift* J195509.6+261406, including data from P60(black), Keck/LRIS (black), and the literature (grey). (French et al. 2007; de Ugarte Postigo et al. 2007; Kann et al. 2007b; Updike et al. 2007a; Stefanescu et al. 2007a; Yoshida et al. 2007; Klotz et al. 2007; Stefanescu et al. 2007c; Updike et al. 2007b).

TABLE 2
OPTICAL OBSERVATIONS OF *Swift* J195509.6+261406 AT KECK

Mean Epoch (2007 UT)	Facility	Filter	Exposure (s)	Magnitude (s)
Jun 13.570	LRIS	<i>I</i>	120 × 3	> 24.0
Jun 15.517	LRIS	<i>I</i>	200 × 3	24.37 ± 0.21
Jun 15.524	LRIS	<i>R</i>	180 × 1	22.25 ± 0.06
Jun 15.527	LRIS	<i>R</i>	180 × 1	24.21 ± 0.13
Jun 15.531	LRIS	<i>R</i>	180 × 1	23.28 ± 0.07
Jun 15.534	LRIS	<i>R</i>	180 × 1	24.09 ± 0.11

NOTE. — Error quoted are $1-\sigma$ photometric and instrumental errors summed in quadrature. Upper limits quote are $3-\sigma$. No correction has been made for the large (and uncertain) line-of-sight extinction.

Astronomers using other facilities – including the OSN 1.5-m telescope (de Ugarte Postigo et al. 2007), the 2-m Schmidt telescope of the Thüringer Landessternwarte (Kann et al. 2007b), the 25-cm *TAROT* facility (Klotz et al. 2007), and the 40-cm *Watcher* telescope (French et al. 2007) – confirmed the detection of this variable source. Detections and upper limits reported to the GRB Coordinates Network (GCN) are shown in Figure 6.

Drawn by the excitement of these discoveries, we began monitoring the field of *Swift* J195509.6+261406 in the i' filter with the automated Palomar 60-inch telescope (P60; Cenko et al. 2006) starting at 5:47 UT 2007 June 12 and continued over the next several nights. In addition, we imaged the field in *R*-, *I*- and *g*- bands with the *Low Resolution Imaging Spectrograph* (LRIS; Oke et al. 1995) mounted at the Cassegrain focus of the Keck I 10-m telescope. All images were reduced using standard IRAF¹⁸ routines.

¹⁸ IRAF is distributed by the National Optical Astronomy Observatory, which is operated by the Association for Research in Astronomy, Inc., under cooperative agreement with the National Science Foundation.

The light curve obtained from observations reported via GCN¹⁹ and our data are summarized in Figure 6. The P60 and the Keck photometry can be found in Table 5 and Table 2 respectively.

The P60 light curve is dominated by flickering and magnificent flares on the night of 2007 June 12 (see Figure 7). We observed over eleven flares with amplitudes greater than one magnitude in only three hours. The brightest of these flares rose and dropped by more than 3.5 magnitudes within 6 minutes. The amplitude of the flares is a lower limit because the P60 images are not deep enough to detect the quiescent counterpart (see below). The timescale is also an upper limit because it is entirely possible that variability is more rapid than our sampling rate (~ 60 s). If we define duty-cycle as the fraction of time for which the *Swift* J195509.6+261406 was brighter than i' , then the duty cycle based on the first night of data is 18.6%. Given that there was no detection on subsequent ten nights, the duty cycle reduces to 5.8%.

We see a dramatic flare in the *LRIS* data five days (2007 June 15) after the high-energy emission, even though the transient is at a much fainter quiescent magnitude. The brightest observed flare in *R*-band was 2 magnitudes in three minutes (see Figure 8). Much like the behavior seen in X-rays (§2), such dramatic optical variability at late times is unlike anything seen before from an extragalactic GRB optical afterglow. Unfortunately none of our optical data directly overlap the XRT light curve, making a direct correlation between the two impossible.

4. A NEAR INFRARED COUNTERPART

Given the large line-of-sight extinction, we undertook late-time NIR imaging at a variety of facilities to search for a quiescent counterpart to *Swift* J195509.6+261406. The results of our campaign are summarized in Table 3.

In detail, we observed the field of *Swift* J195509.6+261406 with the Near InfraRed Imager and spectrograph (NIRI; Hodapp et al. 2003) mounted on the 10-m Gemini North telescope on two occasions. On 2007 June 19 we obtained 18×60 s images in the *K*-band under exquisite seeing ($\sim 0.4''$) and photometric conditions. The observations on 2007 July 15 suffered from poor seeing and clouds.

On 2007 June 21, starting 13:10 UT, we observed the transient with Laser Guide Star Adaptive Optics (LGS-AO; Wizinowich et al. 2006; van Dam et al. 2006) on the Keck II telescope and the Near-Infrared Camera 2 (NIRC2). A total of 17 images were obtained, each consisting of three 20s co-added integrations, in the *K'* filter using the wide-angle camera.

Finally, *J*- and *H*-band images were obtained with the Wide-Field Infrared Camera (WIRC; Wilson et al. 2003) mounted on the Palomar Hale 200-inch (P200) telescope. Thirty four images each with integration time of 30 s were taken in each filter on the night of 21 June 2007.

All but the LGS data were processed with standard IRAF routines. Custom routines in *Python* and *IDL* (written by JSB and LP) were used for the LGS-AO reductions; a custom distortion correction (obtained by PBC) was applied to the LGS-AO imaging. We created

¹⁹ http://gcn.gsfc.nasa.gov/gcn3_archive.html

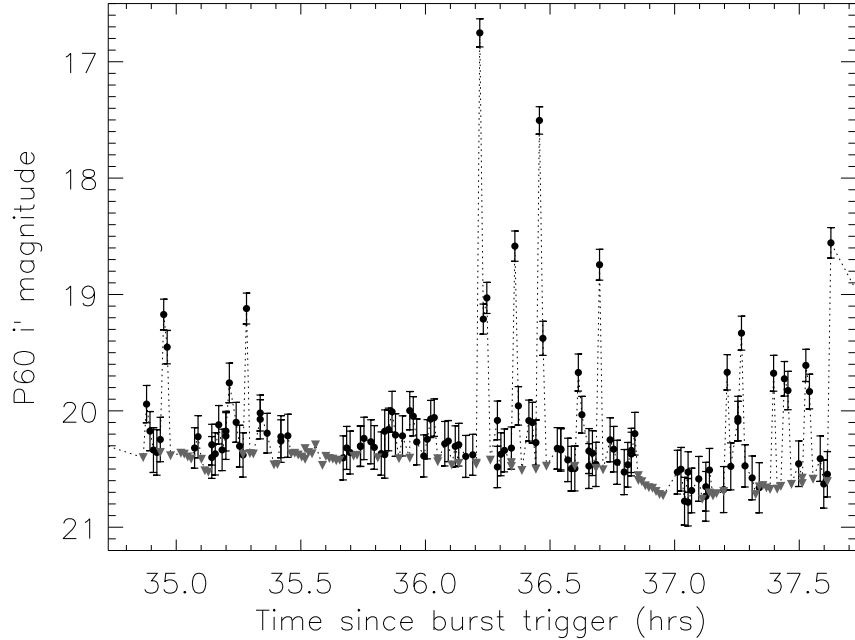


FIG. 7.— P60 i' -band light curve from the night of 2007 June 12. Upper limits are indicated by grey inverted triangles. The rapid variability (time scales less than 60 s, our sampling rate) at late times is unlike any previous long-duration GRB optical afterglow.

an astrometric solution using our Gemini/NIRI K -band image from the night of June 19 relative to about fifty point sources from the $2\text{-}\mu\text{m All-Sky Survey}$ ($2MASS$; Skrutskie et al. 2006). The resulting RMS positional uncertainty was $0.125''$ in right ascension and $0.098''$ in declination. This NIRI K -band image was then used to create a catalog of about one hundred point sources for astrometric matching with all other images. The NIRI K -band image was chosen because of the excellent seeing conditions ($\sim 0.4''$) and the larger field of view in comparison to NIRC2. Typical RMS positional uncertainties relative to the reference image were $\approx 0.07''$ in each coordinate. Using these astrometric solutions, we determine a position for the optical transient in the Keck R -band flares of $\alpha = 19^{\text{h}}55^{\text{m}}09.^{\text{s}}646$, $\delta = +26^{\circ}14'05.^{\prime\prime}62$ (J2000.0).

At the location of the $LRIS$ optical transient, we find a single point source in our LGS-AO/NIRC2 and the first epoch of NIRI imaging (see Figure 9). Despite the presence of two nearby objects (A and B , see Figure 9), our astrometric accuracy is sufficient to unambiguously identify this K -band source with the optical transient. Using the LGS-AO/NIRC2 image, we find that the location of the NIR counterpart is $\alpha = 19^{\text{h}}55^{\text{m}}9.^{\text{s}}649$, $\delta = +26^{\circ}14'5.^{\prime\prime}65$ (J2000.0), with an uncertainty of 100 mas in each direction.

Due to the crowded field, PSF-matched photometry was performed on all images using the IRAF DAOPHOT package. The K -band counterpart shows marginal evidence for fading between the NIRI and LGS observations (Table 3); however our photometric uncertainty may have been underestimated given some degree of contamination in the NIRI images. For reference, the $RIJHK_s$ magnitudes of objects A and B are provided in Table 4.

TABLE 3
NIR OBSERVATIONS OF $Swift$ J195509.6+261406

Epoch (2007 UT)	Facility	Filter	Magnitude
Jun 19.549	Gemini-N/NIRI	K	19.30 ± 0.23
Jun 21.220	Keck II/LGS-AO+NIRC2	K'	19.83 ± 0.15
Jul 15.309	Gemini-N/NIRI	K	> 19.5
Jun 21.352	P200/WIRC	J	> 20.5
Jun 21.400	P200/WIRC	H	> 19.5

NOTE. — Errors quoted are $1\text{-}\sigma$ photometric and instrumental errors summed in quadrature. Upper limits quoted are $3\text{-}\sigma$. No correction has been made for the large (and uncertain) line-of-sight extinction.

TABLE 4
PHOTOMETRY OF NEARBY CONTAMINATING SOURCES A AND B

Epoch (2007 UT)	Facility	Filter	Magnitude Source A	Magnitude Source B
Jun 15.594	Keck I/LRIS	R	> 25.0	> 25.0
Jun 15.517	Keck I/LRIS	I	24.83 ± 0.21	24.93 ± 0.22
Jun 21.352	P200/WIRC	J	> 20.5	> 20.5
Jun 21.400	P200/WIRC	H	> 19.5	> 19.5
Jun 21.220	Keck II/LGS	K'	20.30 ± 0.16	19.44 ± 0.14

NOTE. — Source B is 471 ± 22 mas West and 670 ± 22 mas South of $Swift$ J195509.6+261406. In images with poorer angular resolution, stars A and B may contaminate the photometry of the transient (i.e. our NIRI imaging). Errors quoted are $1\text{-}\sigma$ photometric and instrumental errors summed in quadrature. Upper limits quoted are $3\text{-}\sigma$. No correction has been made for the large (and uncertain) line-of-sight extinction.

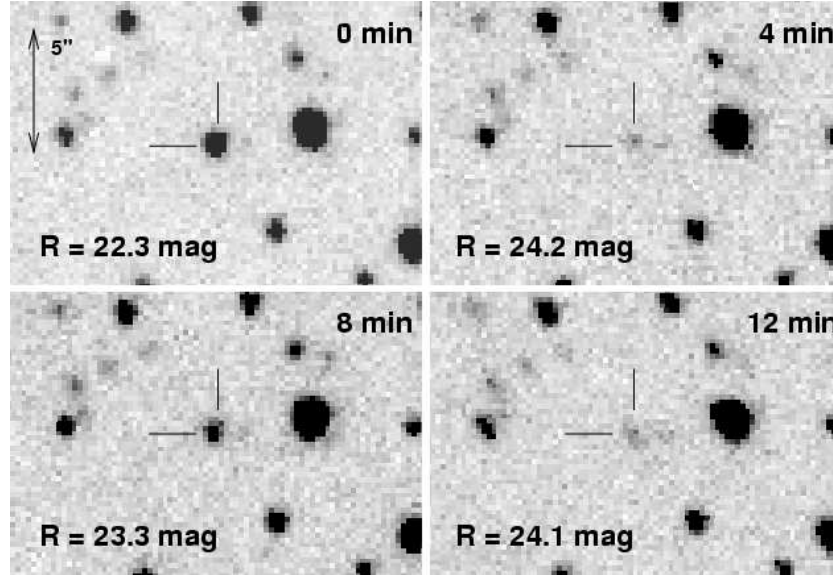


FIG. 8.— Close up view of the optical field of the *Swift* J195509.6+261406 optical transient using the *LRIS* instrument on the Keck I 10-m telescope; 2007 June 15 starting at 12:33 UT. All four images were taken in the *R*-band with a 180 s exposure in sequence. The transient brightens by over two magnitudes in only three minutes about five days after the burst trigger. Such rapid variability at late times is unprecedented from an extragalactic GRB optical afterglow.

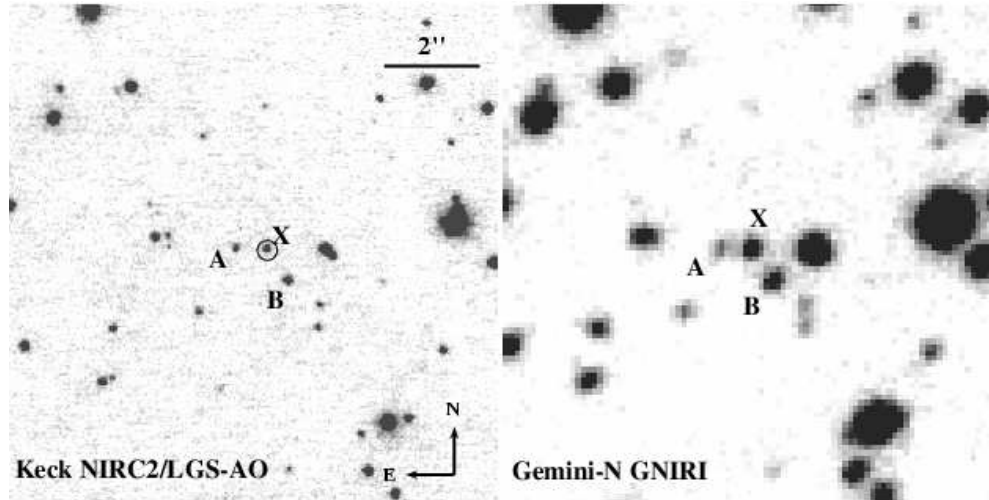


FIG. 9.— A *K*-band image of the field of *Swift* J195509.6+261406 obtained with NIRC-2 imager behind the Keck II Laser Guide Star (LGS) system (left; 2007 June 21) and NIRI imager on the Gemini-North telescope (right; 2007 June 19). The 2σ error circle of the optical transient (taken from our *LRIS* imaging) is shown as a black circle overlaid on the LGS image. Clearly we can identify the object marked as 'X' as the NIR counterpart of *Swift* J195509.6+261406.

5. SEARCH FOR A RADIO COUNTERPART

On 2007 June 15 we undertook Very Large Array (VLA)²⁰ observations of *Swift* J195509.6+261406. The observations were obtained in 2×50 MHz bands around 8.46 GHz and lasted about an hour.

We observed 1956+283 (a phase calibrator) for 0.8 minutes and then switched to *Swift* J195509.6+261406 for 4.8 minutes. The sequence ended with a 6-minute observation of 0137+331 (3C48; flux calibrator).

Data were analyzed using the Astronomical Image Processing System (AIPS) software of National Radio

Astronomy Observatory (NRAO). VLA antennas N16, W64, E72 and W48 and baseline combinations EVLA antennas E16 W24, N64, W40, E56, W48 and N40 were flagged. In total, flagging resulted in a loss of about 100 baselines.

Owing to the VLA being in the "A" configuration, we obtained excellent image resolution of $0.42'' \times 0.21''$. However, *Swift* J195509.6+261406 was not detected and we get an upper limit of $7.3 \pm 31.5 \mu\text{Jy}$.

6. A K STAR

We obtained optical spectra of *Swift* J195509.6+261406 on June 13.6 and June 15.5 using LRIS. Both nights suffered from clouds. We used the

²⁰ The National Radio Astronomy Observatory is a facility of the National Science Foundation operated under cooperative agreement by Associated Universities, Inc.

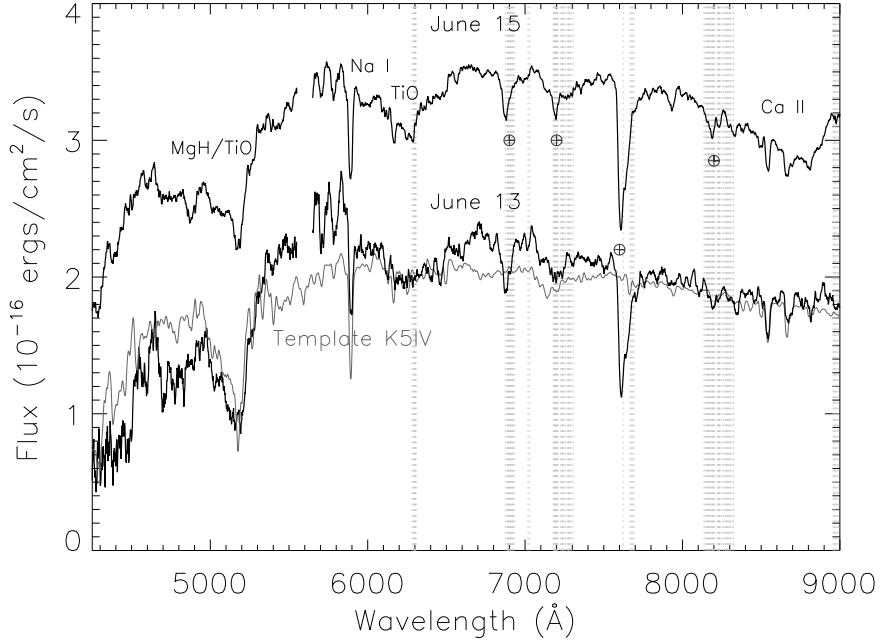


FIG. 10.— Keck LRIS Spectrum. We see no emission lines but many absorption lines prominent in a K star, in particular, TiO bands, Ca II triplet and Na I doublet. Overplotted (grey line) is a template K5IV star with $T=4250\text{K}$, $\log g = 4.0$. The June 15 spectrum is offset from the June 13 spectrum for clarity. The dotted lines mark the position of atmospheric lines. The break in the spectrum is due to the dichroic cross-over.

400/8500²¹ grating and 400/3400 grism with a dichroic at 5600, thereby covering a range of 4000–9000 Å. Data were reduced using IRAF. The extinction estimate based on the full X-ray spectrum excluding the flare (see Table 1) corresponds to $E(B-V) = 1.0\text{--}1.5$. We use the extinction curve described by Cardelli et al. (1989) with $R = 3.1$ to de-redden the spectra.

We compared our spectra to synthetic spectra based on Kurucz's codes with resolution of 11500 (Munari et al. 2005)²². After marking the atmospheric bands, we identify the prominent absorption features as Na D (5890 Å), Ca II triplet (8500, 8542, 8660 Å), broad TiO (4954–5200 Å) and MgH (5180 Å). The fundamental physical parameters are temperature, gravity and metallicity. The extrinsic unknown is the interstellar extinction, $E(B-V)$. We compared a number of spectra obtained by varying these four parameters. Unfortunately it appears that there is a degeneracy between temperature and extinction as well as gravity and metallicity. Assuming solar metallicity and extinction $E(B-V)$ of 1.1, we find that the best fit to *Swift* J195509.6+261406 is spectral type K5IV or K2III. Since the spectra are low resolution and the extinction is uncertain, we can't infer the physical parameters very precisely.

However, we obtain the following constraints. We eliminate stars of spectral type M0 and colder based on the absence of TiO bands. We rule out supergiants based on the relatively shallow depth of the Ca II triplet of our observed spectrum compared to the model. Sim-

ilarly, we also rule out dwarfs hotter than K5 due to the relatively deep depth of Ca II. The Na I doublet is a less reliable diagnostic due to possible contamination from the interstellar medium. We constrain the temperature to 4000–4500 K and $\log(g) > 2.0$. Using Cox (2000), this corresponds to a mass of $0.7\text{--}1.2 M_{\odot}$ and radius of $1\text{--}25 R_{\odot}$. In terms of absolute K magnitude, a K5V star has $M_K = 4.5$ magnitude and a K2III star has $M_K = -2.2$ magnitude. Thus, we cannot use the spectra to constrain the distance to the source.

Given that observations were obtained under cloudy conditions we used a bright star along the slit for relative flux calibration in addition to a usual flux calibrator. Although the second epoch was obtained immediately after a high amplitude flare (see Figure 8) and the first epoch during relative quiescence, we find that the optical transient (star X in Figure 9) is $\sim 20\%$ brighter on the second epoch. This suggests that the timescale of variability is short and doesn't contribute to our 40-minute integration.

Since we used slit widths of $1.5''$ on June 13 and $1.0''$ and chose a position angle of 6° east of north, we consider the possibility of contamination by stars A and B (see Figure 9). We calculate the median of our two-dimensional spectra along the dispersion axis but find no asymmetry in the PSF. Moreover, relative to the optical transient, source A and B are fainter in I band by ~ 0.5 mag and undetected in R band. Source A is fainter in K' by ~ 0.5 mag and Source B is brighter by ~ 0.4 mag. Both are undetected in J and H bands (see Table 4). If we compare the $K - I$ colors, Source B is redder than star X and Source A by 1 magnitude. Given the faintness and redness, we conclude that the contamination

²¹ Gratings are labeled by the convention n/m where n is the number of lines of ruling per mm and m is the blaze wavelength

²² <http://gaia.esa.int/spectralib/spectralib1A/SpectraLib1a.cfm>

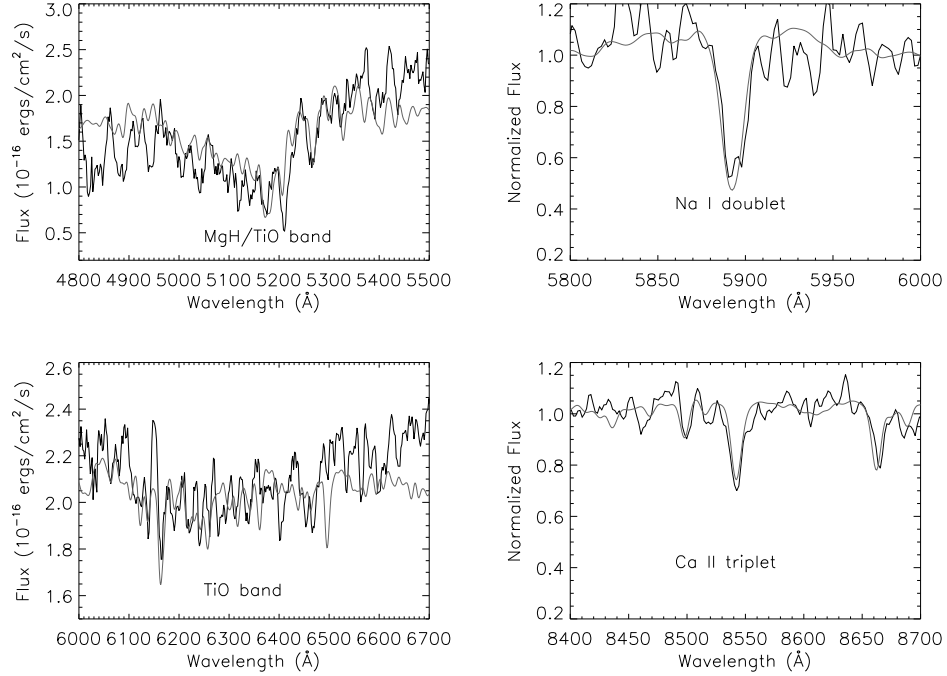


FIG. 11.— June 13 LRIS Spectra around specific temperature and gravity indicators. Overplotted in grey is a K5IV synthetic template. On the left are the broad TiO bands shown in flux units to emphasize the morphology. On the right is the Na I doublet and Ca II triplet normalized relative to the continuum to emphasize the depth and width of line.

fraction to our spectrum by these sources is minimal.

7. ARCHIVAL OBSERVATIONS

A query of the *Simbad* database reveals no catalogued object within the BAT localization. The INTEGRAL observatory conducts regular scans of the Galactic plane and, in addition, performed several long pointed observations of the field around *Swift* J195509.6+261406. Over the past four years, this field has been observed with the IBIS telescope to total 1.5 Ms being within its fully-coded field-of-view (FCFOV, $9^\circ \times 9^\circ$) and up to 2.5 Ms being within the partially coded field-of-view (PCFOV, $29^\circ \times 29^\circ$). The efficiency of observations within the FCFOV falls to zero at the field's edge. The coverage of these 4 years by observations was non-uniform with the maximum exposure reached in the fall of 2006 (for FCFOV).

There is no reported source close to the transient's position in the recent IBIS/ISGRI soft gamma-ray catalogs (Krivonos et al. 2007; Bird et al. 2007). We have also reanalyzed the archival data of INTEGRAL and failed to detect the source. A 4- σ limit of 0.9 mCrab in the 18–45 keV band (or 0.8 mCrab in the 17–60 keV band) has been received (flux of 1 mCrab corresponds to 1.1 and 1.4×10^{-11} erg cm $^{-2}$ s $^{-1}$ in these bands respectively for a source with Crab-like spectrum). There was also no source detected on a time scale of one individual pointing (2.0–3.6 ksec). We derive a 4- σ limit of \sim 20 mCrab.

Also, there is no compelling detection on days or weeks timescale with the Rossi X-Ray Timing Explorer All Sky Monitor survey (upper limit of \sim 1 mCrab; 2–10 keV), over more than 10 years of monitoring (R. Remillard, personal communication).

Spitzer observed the position of *Swift*

J195509.6+261406 during the Galactic Legacy Infrared Mid-Plane Survey Extraordinaire (GLIMPSE) on 2004 Oct 31st. Conservative upper limits for a source at the *K*-band position are 280, 350, 1700 and 6350 μ Jy at 3.6, 4.5, 5.8 and 8.0 μ m respectively.

8. BASIC CONSIDERATIONS: DISTANCE, ENERGETICS AND RADIUS

The fluence, the hardness and the duration of GRB 070610 are not atypical of GRBs. However, *Swift* J195509.6+261406 is an atypical afterglow in the X-ray band (§2). The optical counterpart is also atypical. Correcting for the interstellar extinction the apparent *R*-band magnitude of the optical transient is as bright as 13 mag more than a day after the burst trigger – there is no other optical afterglow this bright at such late times (Kann et al. 2007a).

The issue that faces us is quite simple: is GRB 070610 related to *Swift* J195509.6+261406? For extragalactic long-duration GRBs that the *Swift*-XRT was able to observe within an hour of the burst trigger, the overwhelming majority have a detected X-ray afterglow.

We therefore consider it unlikely that GRB 070610 arises from a background (i.e. extragalactic) event. The spatial and temporal coincidence of GRB 070610 and *Swift* J195509.6+261406 suggest that these are strongly related. If so, the event is of Galactic origin with a distance of $10 d_{10}$ kpc.

Accepting this association we turn our attention to the fundamental parameters characterizing *Swift* J195509.6+261406. The infrared *K*-band magnitude of the NIR counterpart *Swift* J195509.6+261406 is no brighter than \sim 19.8 (Table 3). A K5-K7 dwarf has $M_K = 4.5\text{--}4.7$ (Cox 2000). Thus, assuming no line-of-sight

extinction and assuming it is a K5V, we get an upper limit on the distance of $d \lesssim 11$ kpc. But, as noted in §6, if the star is a giant, we cannot put a useful constraint on the distance since the star would be outside our galaxy.

The prompt γ -ray burst peak flux is 5×10^{-8} erg cm $^{-2}$ s $^{-1}$, the peak X-ray flare flux is twice as faint and the mean flux over the first week is approximately a factor of 10^4 fainter than the burst peak flux. These translate to the following isotropic luminosities: $6 \times 10^{38} d_{10}^2$ erg s $^{-1}$, $3 \times 10^{38} d_{10}^2$ erg s $^{-1}$ and $5 \times 10^{34} d_{10}^2$ erg s $^{-1}$.

The prompt gamma-rays can constrain the radius of the emission. The BAT burst duration of several seconds (see Figure 1) puts an upper limit on the size of the emitting region (along the line of sight) to be smaller than $\sim 10^{11} \beta_c$ cm, where β_c is the causal speed in units of the light speed (i.e., the speed in which information, such as sound, travels). Since we expect $\beta_c \ll 1$ in non-compact objects (e.g., main sequence stars) the source of the prompt gamma-rays is a black hole, a neutron star or a white dwarf (the sound crossing time of the latter is seconds).

On the other hand, the non-thermal gamma-rays can be used to put a lower limit on the emission radius. If the gamma-ray spectrum continues to high energy ($E > m_e c^2$) then pair production opacity starts playing a role. Using the formulation of Lithwick & Sari (2001) and assuming a non-relativistic source we find that the size of the emitting region has to be $\gtrsim L\sigma_T/(0.1\pi m_e c^3) \approx 10^9 d_{10}^2$ cm, where the approximated numerical factor (taken here as 0.1π) depends on the radiation spectrum and the geometry of the source (Svensson 1987). This radius implies that if the engine of the burst is a neutron star or a black hole then the observed gamma-rays are produced far from the engine by (possibly relativistic) ejecta.

9. A CURIOUS GALACTIC TRANSIENT

With a compact object (§8) and a quiescent K-star companion (§6), *Swift* J195509.6+261406 is almost certainly a binary system. We now turn our attention to investigate the mechanism powering the unusual emission, with an emphasis on identifying analogous systems in our Galaxy.

At first blush, soft γ -ray repeater (SGR) flares appear to be a viable model for *Swift* J195509.6+261406. SGR exhibits hard X-ray flares with durations ranging from 0.1s to 10s and isotropic luminosities of 10^{46} erg (Aptekar et al. 2001; Hurley et al. 2005). Furthermore, variable X-ray afterglows have been detected after several SGR outbursts (see e.g. Woods & Thompson 2006).

However, this interpretation has several problems. First, SGR flares lasting longer than 1s, dubbed “intermediate” SGR flares, have an energy release $\approx 10^{41}$ erg, two orders of magnitude larger than our upper limit for *Swift* J195509.6+261406 (Woods & Thompson 2006). Second, pulsations are typically observed in SGR flare X-ray afterglows at the neutron star spin rate. We see no evidence for pulsations from *Swift* J195509.6+261406 (though constrained by the 2.5s sampling interval). Finally, no known SGR has a companion. If *Swift* J195509.6+261406 were caused by an SGR flare, the passive K-star companion would make *Swift*

J195509.6+261406 the first binary magnetar.

Unlike SGR flares, the remaining possibilities are ultimately powered by accretion instead of magnetic activity (Arefiev et al. 2003 provides a comprehensive review of such transients in the hard X-ray sky). The *INTEGRAL* mission has identified a class of bright hard X-ray transients, the so-called Supergiant Fast X-ray Transients (SFXT; Negueruela et al. 2007). However, these events are relatively soft, and have timescales of 10^3 s or longer. Furthermore, the super-giant donor is an essential part of the SFXT story – the X-ray flares arise from accretion of “blobs” in the wind of the supergiant star. While the companion star to *Swift* J195509.6+261406 may be a giant, we can definitively rule out a supergiant.

The high peak luminosity strongly suggests an event like CI Cam (see Belloni et al. 1999). However, this too is a questionable analog for the reasons of the lack of a bright optical/NIR counterpart and also the short flare duration. For the same reasons, the analogy to A0538–66 (the well known Be-pulsar X-ray binary in the LMC) can also be ruled out.

The bursting pulsar GRO J1744–28 shares some properties with those from GRB 070610. From 1995–1997, thousands of bursts were detected by BATSE out to > 60 keV (Kouveliotou et al. 1996; Woods et al. 1999). The spectrum of the bursts in BATSE and RXTE was adequately modeled by a thermal bremsstrahlung model having $kT \sim 10$ keV; burst durations were approximately 10s. GRO J1744–28 consists of a neutron star in an 11.8d orbit with a low mass companion (Finger et al. 1996). However, unlike *Swift* J195509.6+261406, there is no evidence for a highly variable optical emission associated with these bursts. Also the high-energy bursts from GRO J1744–28 are highly repetitive. Searches for other episodes of emission from GRB 070610 did not yield any obvious candidates either in the BAT data or in the extensive INTEGRAL survey (§7) and the Interplanetary Network (§10).

The best analog to the X-ray and optical emission from *Swift* J195509.6+261406 is V4641 Sgr (Markwardt et al. 2007) – a transient which has been recognized by several authors as being one of the fastest transients in the hard X-ray (in’t Zand et al. 2000; Uemura et al. 2002; Arefiev et al. 2003). V4641 Sgr came to the attention of astronomers through a major outburst in 1999 (see in’t Zand et al. 2000). We now know that this object is a binary consisting of a B9 III star orbiting a $9 M_\odot$ black hole (Orosz et al. 2001). The system exhibited strong and fast X-ray and optical variability – similar to what we see in *Swift* J195509.6+261406.

Rapid (100s or shorter) and intense (modulation index, $S = \langle f \rangle / \Delta(f) \gtrsim 10$; here f is the X-ray flux and Δf is the variability in f) but with mean X-ray luminosity $\langle L \rangle$ that is well below Eddington flux mark V4641 Sgr from the other black hole binaries (Revnivtsev et al. 2002). The classical black hole LMXBs such as A0620–00 exhibit X-ray novae with peak super-Eddington flux and a decline over a month (see reviews by Tanaka & Shibasaki 1996; Remillard & McClintock 2006). Micro-quasars such as GRS 1915+10 exhibit intense variations (with S approaching ten) but only when $\langle L \rangle$ is extremely high, $\langle L \rangle \sim 10^{39}$ erg s $^{-1}$ (e.g. Belloni et al. 1997; Munoz et al. 1999).

The first difference between *Swift* J195509.6+261406 and V4641 Sgr is the donor star: *Swift* J195509.6+261406 has a K-star donor, while V4641 Sgr has a B9 donor. We suggest that the distinctive variability of V4641 Sgr arises from the black hole companion and has less to do with the nature of the donor star. This conjecture would allow us to infer that the compact object in *Swift* J195509.6+261406 is also a black hole. While V4641 Sgr seems to be the closest event we have to *Swift* J195509.6+261406, it is clear that no perfect analog to *Swift* J195509.6+261406 exists. In particular, there has been no report of a burst of gamma rays from V4641 Sgr. However, the absence could be due to the short duration duty cycle of the gamma ray bursts.

With two similar objects in hand—V4641 Sgr and GRB 070610—we now have the luxury of defining a new class of transients: fast X-ray novae which, in addition to the rapid X-ray and optical variability but at sub-Eddington luminosities, are also (apparently) marked by GRB-like bursts.

What differentiates fast X-ray novae from the regular X-ray novae? Regular X-ray novae are essentially black hole binaries undergoing the equivalent of dwarf novae i.e. instabilities in the disk. During the major burst of 1999, V4641 Sgr exhibited radio emission and relativistic motion (Hjellming et al. 2000). According to Orosz et al. 2001, the distance to V4641 Sgr is 7.4–12.3 kpc and the apparent expansion velocity is $> 9.5c$ —making V4641 Sgr the most relativistic of Galactic sources. This suggests that perhaps the key difference between fast X-ray novae and the regular X-ray novae is the speed at which the ejecta is emitted. (Unfortunately our radio observations were not undertaken immediately after the detection of GRB 070610.)

10. IMPLICATIONS: GALACTIC GRBS

Spurred by the connection between *Swift* J195509.6+261406 with a Galactic transient we investigated whether this source or its analog V4641 Sgr emitted bursts of gamma-rays in the past. We have constructed a list of 1211 GRBs detected by the IPN (Hurley et al. 1999), whose position is constrained by at least one annulus with semi-width smaller than 0.5 deg. This catalog contains events observed from 1990 November 12, to 2005 October 31 (see Ofek 2007 for more details). We did not find any IPN GRB that coincides with either of these positions.

We also searched for *Swift*-BAT sub-threshold events which are consistent with the positions of V4641 Sgr and *Swift* J195509.6+261406. There is no BAT sub-threshold event within 5' from the location of V4641 Sgr. But, we find an event at a signal-to-noise ratio (SNR) of 5.0 located at RA=298.77°, Dec=+26.221° (1.8' from the position of GRB 070610) and occurring on UT 2006 Nov 17.7812. However, adjusted for the approximate number of times this field has been observed, the significance drops below 2- σ . We consider it likely this sub-threshold event is nothing more than a statistical fluctuation.

V4641 Sgr has been undergoing major bursts approximately every two years (see Uemura et al. 2004). The absence of a detection of a gamma-ray burst could simply be due to lack of coverage or that not all such bursting activity are preceded by a burst of gamma-rays.

Another possible member of this class of fast

X-ray novae is XTEJ1901+014 (Karasev et al. 2007) which is potentially associated with GRB020406 (Remillard & Smith 2002).

Nonetheless, it is reasonable to speculate that a burst similar to *Swift* J195509.6+261406 occurs in our Galaxy, say, every decade. This alone immediately makes *Swift* J195509.6+261406 and related events as the most common of long-duration gamma-ray bursts. (The mean time between cosmological GRBs in our Galaxy is no smaller than 10^5 yr).

Several hundred years ago, optical astronomers put all new apparitions of stars as *novae stella*. Over the past century astronomers have shown that *novae stella* split into three distinctly different phenomena: novae, supernovae of type Ia and core collapse supernovae. The novae, in turn, are divided into five families which arise from instabilities in the accretion disk feeding a white dwarf, neutron star or a black hole and on the surfaces of white dwarfs and neutron stars.

History is repeating itself. Only thirty years ago, astronomers referred to all bursts of gamma-ray radiation as GRBs. Over the last decade astronomers have established SHBs and LSBs to be of cosmological origin (Metzger et al. 1997; Gehrels et al. 2005; Bloom et al. 2006; Fox et al. 2005) and reasonably established their origin: coalescence of compact objects and deaths of massive stars respectively.

However, fissures are already developing. Recently, hypergiant flares from magnetars in our own Galaxy and nearby galaxies have been found to contaminate the SHB sample. The Galactic rate of the hypergiant flares is likely 10^{-3} yr $^{-1}$ (Ofek 2007) much larger than the estimated Galactic SHB rate of 10^{-6} yr $^{-1}$ (Nakar et al. 2006; Guetta & Piran 2006).

Our galaxy has at least two fast X-ray novae systems (V4641 Sgr and *Swift* J195509.6+261406). The rate of GRB 070610-like events is likely to be about $3.5^{+8.0}_{-2.9}$ yr $^{-1}$ which is five orders of magnitude larger than the estimated cosmological GRBs rate. As usual the meekest events dominate the demography.

We thank M. van Kerkwijk for help with Keck observations and discussions. We thank J. Cohen, J. Simon and A. Kraus for valuable discussions. We also acknowledge useful discussions with M. Muno, E. S. Phinney and R. Narayan. As always we are grateful to the selfless librarians and astronomers who maintain the *Simbad* database. M. M. K. thanks the Gordon and Betty Moore Foundation for support with the George Ellory Hale Fellowship. S. B. C. and A. M. S. are supported by a NASA Graduate Student Research Fellowship. JSB is a Sloan Research Fellow and is partially supported by a Hellman Faculty Award. P. C. S. is supported by a Jansky Fellowship. E. B. is supported by a Hubble fellowship. GRB research at Caltech is supported in part by grants from NSF (AST program) and NASA (Swift and HST mission).

REFERENCES

- Aptekar, R. L., Frederiks, D. D., Golenetskii, S. V., Il'inskii, V. N., Mazets, E. P., Pal'shin, V. D., Butterworth, P. S., & Cline, T. L. 2001, ApJS, 137, 227
- Arefiev, V. A., Priedhorsky, W. C., & Borozdin, K. N. 2003, ApJ, 586, 1238
- Barthelmy, S. D., Barbier, L. M., Cummings, J. R., Fenimore, E. E., Gehrels, N., Hullinger, D., Krimm, H. A., Markwardt, C. B., Palmer, D. M., Parsons, A., Sato, G., Suzuki, M., Takahashi, T., Tashiro, M., & Tueller, J. 2005, Space Science Reviews, 120, 143
- Belloni, T., Dieters, S., van den Ancker, M. E., Fender, R. P., Fox, D. W., Harmon, B. A., van der Klis, M., Kommers, J. M., Lewin, W. H. G., & van Paradijs, J. 1999, ApJ, 527, 345
- Belloni, T., Mendez, M., King, A. R., van der Klis, M., & van Paradijs, J. 1997, ApJ, 488, L109+
- Bird, A. J., Malizia, A., Bazzano, A., Barlow, E. J., Bassani, L., Hill, A. B., Bélangier, G., Capitanio, F., Clark, D. J., Dean, A. J., Fiocchi, M., Götz, D., Lebrun, F., Molina, M., Produit, N., Renaud, M., Sguera, V., Stephen, J. B., Terrier, R., Ubertini, P., Walter, R., Winkler, C., & Zurita, J. 2007, ApJS, 170, 175
- Bloom, J. S., Prochaska, J. X., Pooley, D., Blake, C. H., Foley, R. J., Jha, S., Ramirez-Ruiz, E., Granot, J., Filippenko, A. V., Sigurdsson, S., Barth, A. J., Chen, H.-W., Cooper, M. C., Falco, E. E., Gal, R. R., Gerke, B. F., Gladders, M. D., Greene, J. E., Hennawi, J., Ho, L. C., Hurley, K., Koester, B. P., Li, W., Lubin, L., Newman, J., Perley, D. A., Squires, G. K., & Wood-Vasey, W. M. 2006, ApJ, 638, 354
- Bucccheri, R., Bennett, K., Bignami, G. F., Bloemen, J. B. G. M., Boriakoff, V., Caraveo, P. A., Hermse, W., Kanbach, G., Manchester, R. N., Masnou, J. L., Mayer-Hasselwander, H. A., Ozel, M. E., Paul, J. A., Sacco, B., Scarsi, L., & Strong, A. W. 1983, A&A, 128, 245
- Burrows, D. N., Hill, J. E., Nosek, J. A., Kennea, J. A., Wells, A., Osborne, J. P., Abbey, A. F., Beardmore, A., Mukerjee, K., Short, A. D. T., Chincarini, G., Campana, S., Citterio, O., Moretti, A., Pagani, C., Tagliaferri, G., Giommi, P., Capalbi, M., Tamburelli, F., Angelini, L., Cusumano, G., Bräuning, H. W., Burkert, W., & Hartner, G. D. 2005, Space Science Reviews, 120, 165
- Cardelli, J. A., Clayton, G. C., & Mathis, J. S. 1989, ApJ, 345, 245
- Cenko, S. B., Fox, D. B., Moon, D.-S., Harrison, F. A., Kulkarni, S. R., Henning, J. R., Guzman, C. D., Bonati, M., Smith, R. M., Thicksten, R. P., Doyle, M. W., Petrie, H. L., Gal-Yam, A., Soderberg, A. M., Anagnostou, N. L., & Laity, A. C. 2006, PASP, 118, 1396
- Chincarini, G., Moretti, A., Romano, P., Falcone, A. D., Morris, D., Racusin, J., Campana, S., Guidorzi, C., Tagliaferri, G., Burrows, D. N., Pagani, C., Stroh, M., Grupe, D., Capalbi, M., Cusumano, G., Gehrels, N., Giommi, P., La Parola, V., Mangano, V., Mineo, T., Nosek, J. A., O'Brien, P. T., Page, K. L., Perri, M., Troja, E., Willingale, R., & Zhang, B. 2007, ArXiv Astrophysics e-prints
- Cox, A. N. 2000, Allen's astrophysical quantities (Allen's astrophysical quantities, 4th ed. Publisher: New York: AIP Press; Springer, 2000. Edited by Arthur N. Cox. ISBN: 0387987460)
- de Ugarte Postigo, A., Castro-Tirado, A. J., Aceituno, F., et al. 2007, GCN Circular 6501
- Dickey, J. M. & Lockman, F. J. 1990, ARA&A, 28, 215
- Evans, P. A., Beardmore, A. P., Page, K. L., Tyler, L. G., Osborne, J. P., Goad, M. R., O'Brien, P. T., Vetere, L., Racusin, J., Morris, D., Burrows, D. N., Capalbi, M., Perri, M., Gehrels, N., & Romano, P. 2007, A&A, 469, 379
- Falcone, A. D., Burrows, D. N., Lazzati, D., Campana, S., Kobayashi, S., Zhang, B., Mészáros, P., Page, K. L., Kennea, J. A., Romano, P., Pagani, C., Angelini, L., Beardmore, A. P., Capalbi, M., Chincarini, G., Cusumano, G., Giommi, P., Goad, M. R., Godet, O., Grupe, D., Hill, J. E., La Parola, V., Mangano, V., Moretti, A., Nosek, J. A., O'Brien, P. T., Osborne, J. P., Perri, M., Tagliaferri, G., Wells, A. A., & Gehrels, N. 2006, ApJ, 641, 1010
- Finger, M. H., Koh, D. T., Nelson, R. W., Prince, T. A., Vaughan, B. A., & Wilson, R. B. 1996, Nature, 381, 291
- Fox, D. B., Frail, D. A., Price, P. A., Kulkarni, S. R., Berger, E., Piran, T., Soderberg, A. M., Cenko, S. B., Cameron, P. B., Gal-Yam, A., Kasliwal, M. M., Moon, D.-S., Harrison, F. A., Nakar, E., Schmidt, B. P., Penprase, B., Chevalier, R. A., Kumar, P., Roth, K., Watson, D., Lee, B. L., Shectman, S., Phillips, M. M., Roth, M., McCarthy, P. J., Rauch, M., Cowie, L., Peterson, B. A., Rich, J., Kawai, N., Aoki, K., Kosugi, G., Totani, T., Park, H.-S., MacFadyen, A., & Hurley, K. C. 2005, Nature, 437, 845
- French, J., Melady, G., Kubanek, P., & Jelinek, M. 2007, GCN Circular 6500
- Gehrels, N., Chincarini, G., Giommi, P., Mason, K. O., Nosek, J. A., Wells, A. A., White, N. E., Barthelmy, S. D., Burrows, D. N., Cominsky, L. R., Hurley, K. C., Marshall, F. E., Mészáros, P., Roming, P. W. A., Angelini, L., Barbier, L. M., Belloni, T., Campana, S., Caraveo, P. A., Chester, M. M., Citterio, O., Cline, T. L., Cropper, M. S., Cummings, J. R., Dean, A. J., Feigelson, E. D., Fenimore, E. E., Frail, D. A., Fruchter, A. S., Garmire, G. P., Gendreau, K., Ghisellini, G., Greiner, J., Hill, J. E., Hunsberger, S. D., Krimm, H. A., Kulkarni, S. R., Kumar, P., Lebrun, F., Lloyd-Ronning, N. M., Markwardt, C. B., Mattson, B. J., Mushotzky, R. F., Norris, J. P., Osborne, J., Paczynski, B., Palmer, D. M., Park, H.-S., Parsons, A. M., Paul, J., Rees, M. J., Reynolds, C. S., Rhoads, J. E., Sasseen, T. P., Schaefer, B. E., Short, A. T., Smale, A. P., Smith, I. A., Stella, L., Tagliaferri, G., Takahashi, T., Tashiro, M., Townsley, L. K., Tueller, J., Turner, M. J. L., Vietri, M., Voges, W., Ward, M. J., Willingale, R., Zerbi, F. M., & Zhang, W. W. 2004, ApJ, 611, 1005
- Gehrels, N., Sarazin, C. L., O'Brien, P. T., Zhang, B., Barbier, L., Barthelmy, S. D., Blustin, A., Burrows, D. N., Cannizzo, J., Cummings, J. R., Goad, M., Holland, S. T., Hurkett, C. P., Kennea, J. A., Levan, A., Markwardt, C. B., Mason, K. O., Meszaros, P., Page, M., Palmer, D. M., Rol, E., Sakamoto, T., Willingale, R., Angelini, L., Beardmore, A., Boyd, P. T., Breeveld, A., Campana, S., Chester, M. M., Chincarini, G., Cominsky, L. R., Cusumano, G., de Pasquale, M., Fenimore, E. E., Giommi, P., Gronwall, C., Grupe, D., Hill, J. E., Hinshaw, D., Hjorth, J., Hullinger, D., Hurley, K. C., Klose, S., Kobayashi, S., Kouveliotou, C., Krimm, H. A., Mangano, V., Marshall, F. E., McGowan, K., Moretti, A., Mushotzky, R. F., Nakazawa, K., Norris, J. P., Nosek, J. A., Osborne, J. P., Page, K., Parsons, A. M., Patel, S., Perri, M., Poole, T., Romano, P., Roming, P. W. A., Rosen, S., Sato, G., Schady, P., Smale, A. P., Sollerman, J., Starling, R., Still, M., Suzuki, M., Tagliaferri, G., Takahashi, T., Tashiro, M., Tueller, J., Wells, A. A., White, N. E., & Wijers, R. A. M. J. 2005, Nature, 437, 851
- Guetta, D. & Piran, T. 2006, A&A, 453, 823
- Hjellming, R. M., Rupen, M. P., Hunstead, R. W., Campbell-Wilson, D., Mioduszewski, A. J., Gaensler, B. M., Smith, D. A., Sault, R. J., Fender, R. P., Spencer, R. E., de la Force, C. J., Richards, A. M. S., Garrington, S. T., Trushkin, S. A., Ghigo, F. D., Waltman, E. B., & McCollough, M. 2000, ApJ, 544, 977
- Hodapp, K. W., Jensen, J. B., Irwin, E. M., Yamada, H., Chung, R., Fletcher, K., Robertson, L., Hora, J. L., Simons, D. A., Mays, W., Nolan, R., Bec, M., Merrill, M., & Fowler, A. M. 2003, PASP, 115, 1388
- Hurley, K., Briggs, M. S., Kippen, R. M., Kouveliotou, C., Meegan, C., Fishman, G., Cline, T., & Boer, M. 1999, ApJS, 120, 399
- Hurley, K., Boggs, S. E., Smith, D. M., Duncan, R. C., Lin, R., Zoglauer, A., Krucker, S., Hurford, G., Hudson, H., Wigger, C., Hajdas, W., Thompson, C., Mitrofanov, I., Sanin, A., Boynton, W., Fellows, C., von Kienlin, A., Lichti, G., Rau, A., & Cline, T. 2005, Nature, 434, 1098
- in't Zand, J. J. M., Kuulkers, E., Bazzano, A., Cornelisse, R., Cocchi, M., Heise, J., Muller, J. M., Natalucci, L., Smith, M. J. S., & Ubertini, P. 2000, A&A, 357, 520
- Kalberla, P. M. W., Burton, W. B., Hartmann, D., Arnal, E. M., Bajaja, E., Morras, R., & Pöppel, W. G. L. 2005, A&A, 440, 775
- Kann, D. A., Wilson, A. C., Schulze, S., Klose, S., Henze, M., Ludwig, F., Laux, U., & Greiner, J. 2007a, GCN Circular 6505
- Kann, D. A., Wilson, A. C., Schulze, S., et al. 2007b, GCN Circular 6505
- Karasev, D. I., Lutovinov, A. A., & Grebenev, S. A. 2007, Astronomy Letters, 33, 159
- Klotz, A., Boer, M., Atteia, J.-L., et al. 2007, GCN Circular 6513
- Kouveliotou, C., van Paradijs, J., Fishman, G. J., Briggs, M. S., Kommers, J., Harmon, B. A., Meegan, C. A., & Lewin, W. H. G. 1996, Nature, 379, 799
- Kravonos, R., Revnivtsev, M., Lutovinov, A., Sazonov, S., Churazov, E., & Sunyaev, R. 2007, ArXiv Astrophysics e-prints
- Lithwick, Y. & Sari, R. 2001, ApJ, 555, 540
- Markwardt, C. B., Pagani, C., Evans, P., Gavriil, F. P., Kennea, J. A., Krimm, H. A., Landsman, W., & Marshall, F. E. 2007, The Astronomer's Telegram, 1102, 1
- Metzger, M. R., Djorgovski, S. G., Kulkarni, S. R., Steidel, C. C., Adelberger, K. L., Frail, D. A., Costa, E., & Frontera, F. 1997, Nature, 387, 878
- Munari, U., Sordo, R., Castelli, F., & Zwitter, T. 2005, A&A, 442, 1127

- Muno, M. P., Morgan, E. H., & Remillard, R. A. 1999, ApJ, 527, 321
- Nakar, E., Gal-Yam, A., & Fox, D. B. 2006, ApJ, 650, 281
- Negueruela, I., Smith, D. M., Torrejon, J. M., & Reig, P. 2007, ArXiv e-prints, 704
- Norris, J. P., Nemiroff, R. J., Bonnell, J. T., Scargle, J. D., Kouveliotou, C., Paciesas, W. S., Meegan, C. A., & Fishman, G. J. 1996, ApJ, 459, 393
- Noosek, J. A., Kouveliotou, C., Grupe, D., Page, K. L., Granot, J., Ramirez-Ruiz, E., Patel, S. K., Burrows, D. N., Mangano, V., Barthelmy, S., Beardmore, A. P., Campana, S., Capalbi, M., Chincarini, G., Cusumano, G., Falcone, A. D., Gehrels, N., Giommi, P., Goad, M. R., Godet, O., Hurkett, C. P., Kennea, J. A., Moretti, A., O'Brien, P. T., Osborne, J. P., Romano, P., Tagliaferri, G., & Wells, A. A. 2006, ApJ, 642, 389
- Ofek, E. 2007, in American Astronomical Society Meeting Abstracts, Vol. 210, American Astronomical Society Meeting Abstracts, #41.05+
- Oke, J. B., Cohen, J. G., Carr, M., Cromer, J., Dingizian, A., Harris, F. H., Labrecque, S., Lucinio, R., Schaal, W., Epps, H., & Miller, J. 1995, PASP, 107, 375
- Orosz, J. A., Kuulkers, E., van der Klis, M., McClintock, J. E., Garcia, M. R., Callanan, P. J., Bailyn, C. D., Jain, R. K., & Remillard, R. A. 2001, ApJ, 555, 489
- Pagani, C., Barthelmy, S. D., Cummings, J. R., Gehrels, N., Grupe, D., Holland, S. T., Kennea, J. A., Markwardt, C. B., Marshall, F. E., O'Brien, P. T., Palmer, D. M., Parsons, A. M., Stamatikos, M., & Vetere, L. 2007a, GCN Circular 6489
- Pagani, C., Racusin, J. L., & Kennea, J. A. 2007b, GCN Circular 6506
- Remillard, R. A. & McClintock, J. E. 2006, ARA&A, 44, 49
- Remillard, R. A. & Smith, D. 2002, Atel 88
- Revnivtsev, M., Gilfanov, M., Churazov, E., & Sunyaev, R. 2002, A&A, 391, 1013
- Schlegel, D. J., Finkbeiner, D. P., & Davis, M. 1998, ApJ, 500, 525
- Skrutskie, M. F., Cutri, R. M., Stiening, R., Weinberg, M. D., Schneider, S., Carpenter, J. M., Beichman, C., Capps, R., Chester, T., Elias, J., Huchra, J., Liebert, J., Lonsdale, C., Monet, D. G., Price, S., Seitzer, P., Jarrett, T., Kirkpatrick, J. D., Gizis, J. E., Howard, E., Evans, T., Fowler, J., Fullmer, L., Hurt, R., Light, R., Kopan, E. L., Marsh, K. A., McCallon, H. L., Tam, R., Van Dyk, S., & Wheelock, S. 2006, AJ, 131, 1163
- Stefanescu, A., Slowikowska, A., Kanbach, G., et al. 2007a, GCN Circular 6508
- . 2007b, GCN Circular 6492
- . 2007c, GCN Circular 6532
- Svensson, R. 1987, MNRAS, 227, 403
- Tanaka, Y. & Shibasaki, N. 1996, ARA&A, 34, 607
- Tueller, J., Barbier, L., Barthelmy, S. D., Cummings, J., Fenimore, E., Gehrels, N., Krimm, H., Markwardt, C., Pagani, C., Palmer, D., Parsons, A., Sakamoto, T., Sato, G., Stamatikos, M., & Ukwatta, T. 2007, GCN Circular 6491
- Uemura, M., Kato, T., Ishioka, R., Imada, A., Nogami, D., Monard, B., Cook, L. M., Stublings, R., Kiyota, S., Nelson, P., Beninger, J.-Y., Bolt, G., & Heathcote, B. 2004, PASJ, 56, 823
- Uemura, M., Kato, T., Watanabe, T., Stublings, R., Monard, B., & Kawai, N. 2002, PASJ, 54, 95
- Updike, A. C., Hartmann, D. H., Henson, G., et al. 2007a, GCN Circular 6507
- Updike, A. C., Milne, P. A., Williams, G. G., et al. 2007b, GCN Circular 6536
- van Dam, M. A., Bouchez, A. H., Le Mignant, D., Johansson, E. M., Wizinowich, P. L., Campbell, R. D., Chin, J. C. Y., Hartman, S. K., Lafon, R. E., Stomski, Jr., P. J., & Summers, D. M. 2006, PASP, 118, 310
- Wilson, J. C., Eikenberry, S. S., Henderson, C. P., Hayward, T. L., Carson, J. C., Pirger, B., Barry, D. J., Brandl, B. R., Houck, J. R., Fitzgerald, G. J., & Stolberg, T. M. 2003, in Presented at the Society of Photo-Optical Instrumentation Engineers (SPIE) Conference, Vol. 4841, Instrument Design and Performance for Optical/Infrared Ground-based Telescopes. Edited by Iye, Masanori; Moorwood, Alan F. M. Proceedings of the SPIE, Volume 4841, pp. 451–458 (2003)., ed. M. Iye & A. F. M. Moorwood, 451–458
- Wizinowich, P. L., Chin, J., Johansson, E., Kellner, S., Lafon, R., Le Mignant, D., Neyman, C., Stomski, P., Summers, D., Sumner, R., & van Dam, M. 2006, in Presented at the Society of Photo-Optical Instrumentation Engineers (SPIE) Conference, Vol. 6272, Advances in Adaptive Optics II. Edited by Ellerbroek, Brent L.; Bonaccini Calia, Domenico. Proceedings of the SPIE, Volume 6272, pp. 627209 (2006).
- Woods, P. M., Kouveliotou, C., van Paradijs, J., Briggs, M. S., Wilson, C. A., Deal, K., Harmon, B. A., Fishman, G. J., Lewin, W. H. G., & Kommers, J. 1999, ApJ, 517, 431
- Woods, P. M. & Thompson, C. 2006, Soft gamma repeaters and anomalous X-ray pulsars: magnetar candidates (Compact stellar X-ray sources), 547–586
- Yoshida, M., Yanagisawa, K., Shimizu, Y., et al. 2007, GCN Circular 6512
- Zhang, B., Fan, Y. Z., Dyks, J., Kobayashi, S., Mészáros, P., Burrows, D. N., Noosek, J. A., & Gehrels, N. 2006, ApJ, 642, 354

TABLE 5
OPTICAL OBSERVATIONS OF *Swift* J195509.6+261406 WITH PALOMAR 60-INCH TELESCOPE

Epoch (2007 UT)	Facility	Filter	Time Since Burst (hr)	Exposure (s)	Magnitude
Jun 12.241	P60	i'	32.92	30.0×1	19.1 ± 0.14
Jun 12.242	P60	i'	32.94	30.0×1	>19.8
Jun 12.243	P60	i'	32.96	30.0×3	>19.8
Jun 12.244	P60	i'	32.99	30.0×5	19.7 ± 0.16
Jun 12.245	P60	i'	33.00	30.0×5	19.6 ± 0.15
Jun 12.245	P60	i'	33.02	30.0×5	19.6 ± 0.15
Jun 12.246	P60	i'	33.03	30.0×5	19.7 ± 0.15
Jun 12.246	P60	i'	33.05	30.0×5	>19.8
Jun 12.247	P60	i'	33.06	30.0×5	>19.8
Jun 12.247	P60	i'	33.07	30.0×5	>19.8
Jun 12.248	P60	i'	33.09	30.0×1	>19.8
Jun 12.248	P60	i'	33.09	30.0×5	>19.8
Jun 12.249	P60	i'	33.10	30.0×1	18.9 ± 0.13
Jun 12.249	P60	i'	33.11	30.0×1	18.7 ± 0.12
Jun 12.250	P60	i'	33.13	30.0×1	>19.8
Jun 12.251	P60	i'	33.15	30.0×5	>19.8
Jun 12.251	P60	i'	33.17	30.0×3	19.8 ± 0.18
Jun 12.251	P60	i'	33.17	30.0×5	19.7 ± 0.17
Jun 12.252	P60	i'	33.18	30.0×3	19.7 ± 0.16
Jun 12.252	P60	i'	33.19	30.0×3	19.7 ± 0.16
Jun 12.254	P60	i'	33.22	30.0×5	>19.9
Jun 12.254	P60	i'	33.23	30.0×1	>19.8
Jun 12.254	P60	i'	33.23	30.0×5	>19.9
Jun 12.255	P60	i'	33.25	30.0×1	18.5 ± 0.14
Jun 12.255	P60	i'	33.26	30.0×1	>19.8
Jun 12.256	P60	i'	33.29	30.0×1	>19.9
Jun 12.256	P60	i'	33.29	30.0×3	>19.9
Jun 12.256	P60	i'	33.29	30.0×5	>19.9
Jun 12.257	P60	i'	33.30	30.0×1	19.2 ± 0.15
Jun 12.258	P60	i'	33.32	30.0×1	19.8 ± 0.17
Jun 12.259	P60	i'	33.36	30.0×5	19.9 ± 0.16
Jun 12.260	P60	i'	33.37	30.0×5	>19.9
Jun 12.261	P60	i'	33.39	30.0×5	>19.9
Jun 12.261	P60	i'	33.40	30.0×5	>19.9
Jun 12.262	P60	i'	33.41	30.0×5	>20.0
Jun 12.262	P60	i'	33.43	30.0×5	>20.0
Jun 12.263	P60	i'	33.44	30.0×3	19.9 ± 0.16
Jun 12.263	P60	i'	33.44	30.0×5	>20.0
Jun 12.263	P60	i'	33.45	30.0×3	19.7 ± 0.16
Jun 12.264	P60	i'	33.47	30.0×3	19.6 ± 0.15
Jun 12.264	P60	i'	33.48	30.0×3	19.8 ± 0.16
Jun 12.265	P60	i'	33.50	30.0×3	19.9 ± 0.17
Jun 12.266	P60	i'	33.52	30.0×3	>20.0
Jun 12.266	P60	i'	33.52	30.0×5	19.8 ± 0.16
Jun 12.267	P60	i'	33.55	30.0×1	19.4 ± 0.14
Jun 12.267	P60	i'	33.55	30.0×3	>20.0
Jun 12.267	P60	i'	33.55	30.0×5	19.9 ± 0.16
Jun 12.268	P60	i'	33.58	30.0×3	19.9 ± 0.17
Jun 12.313	P60	i'	34.64	30.0×3	20.2 ± 0.19
Jun 12.322	P60	i'	34.86	30.0×3	>20.4
Jun 12.323	P60	i'	34.88	30.0×3	19.9 ± 0.16
Jun 12.323	P60	i'	34.89	30.0×3	20.1 ± 0.16
Jun 12.324	P60	i'	34.90	30.0×3	20.3 ± 0.19
Jun 12.324	P60	i'	34.92	30.0×3	20.3 ± 0.19
Jun 12.325	P60	i'	34.93	30.0×1	>20.3
Jun 12.325	P60	i'	34.93	30.0×3	20.2 ± 0.19
Jun 12.325	P60	i'	34.94	30.0×1	19.1 ± 0.13
Jun 12.326	P60	i'	34.96	30.0×1	19.4 ± 0.14
Jun 12.327	P60	i'	34.97	30.0×1	>20.3
Jun 12.328	P60	i'	35.01	30.0×5	>20.3
Jun 12.329	P60	i'	35.03	30.0×5	>20.3
Jun 12.329	P60	i'	35.04	30.0×5	>20.3
Jun 12.330	P60	i'	35.05	30.0×5	>20.4
Jun 12.331	P60	i'	35.07	30.0×5	20.3 ± 0.17
Jun 12.331	P60	i'	35.08	30.0×5	20.2 ± 0.18
Jun 12.332	P60	i'	35.10	30.0×5	>20.4
Jun 12.332	P60	i'	35.11	30.0×5	>20.5
Jun 12.333	P60	i'	35.12	30.0×5	>20.5
Jun 12.333	P60	i'	35.14	30.0×3	20.4 ± 0.17
Jun 12.333	P60	i'	35.14	30.0×5	20.2 ± 0.17
Jun 12.334	P60	i'	35.15	30.0×3	20.3 ± 0.18

TABLE 5 — Continued

Epoch (2007 UT)	Facility	Filter	Time Since Burst (hr)	Exposure (s)	Magnitude
Jun 12.335	P60	i'	35.17	30.0×3	20.1 ± 0.16
Jun 12.335	P60	i'	35.18	30.0×3	20.3 ± 0.17
Jun 12.336	P60	i'	35.19	30.0×1	20.2 ± 0.20
Jun 12.336	P60	i'	35.19	30.0×3	20.1 ± 0.17
Jun 12.336	P60	i'	35.21	30.0×1	19.7 ± 0.17
Jun 12.338	P60	i'	35.24	30.0×3	20.0 ± 0.17
Jun 12.338	P60	i'	35.25	30.0×3	20.3 ± 0.17
Jun 12.339	P60	i'	35.26	30.0×1	>20.3
Jun 12.339	P60	i'	35.26	30.0×3	20.3 ± 0.19
Jun 12.339	P60	i'	35.28	30.0×1	19.1 ± 0.13
Jun 12.340	P60	i'	35.29	30.0×1	>20.3
Jun 12.340	P60	i'	35.30	30.0×1	>20.3
Jun 12.342	P60	i'	35.33	30.0×1	20.0 ± 0.16
Jun 12.342	P60	i'	35.33	30.0×3	20.0 ± 0.15
Jun 12.343	P60	i'	35.36	30.0×3	20.1 ± 0.17
Jun 12.344	P60	i'	35.39	30.0×5	>20.4
Jun 12.344	P60	i'	35.40	30.0×5	>20.4
Jun 12.345	P60	i'	35.42	30.0×3	20.2 ± 0.18
Jun 12.345	P60	i'	35.42	30.0×5	20.2 ± 0.18
Jun 12.346	P60	i'	35.44	30.0×5	20.2 ± 0.18
Jun 12.347	P60	i'	35.46	30.0×5	>20.3
Jun 12.347	P60	i'	35.47	30.0×5	>20.3
Jun 12.348	P60	i'	35.48	30.0×5	>20.3
Jun 12.349	P60	i'	35.50	30.0×5	>20.3
Jun 12.349	P60	i'	35.51	30.0×1	>20.3
Jun 12.349	P60	i'	35.51	30.0×5	>20.4
Jun 12.350	P60	i'	35.53	30.0×1	>20.3
Jun 12.350	P60	i'	35.54	30.0×1	>20.3
Jun 12.351	P60	i'	35.55	30.0×1	>20.2
Jun 12.352	P60	i'	35.58	30.0×5	>20.4
Jun 12.353	P60	i'	35.60	30.0×5	>20.3
Jun 12.353	P60	i'	35.61	30.0×5	>20.4
Jun 12.354	P60	i'	35.62	30.0×5	>20.4
Jun 12.354	P60	i'	35.64	30.0×5	>20.4
Jun 12.355	P60	i'	35.65	30.0×5	>20.4
Jun 12.355	P60	i'	35.66	30.0×5	20.4 ± 0.18
Jun 12.356	P60	i'	35.68	30.0×5	20.3 ± 0.18
Jun 12.357	P60	i'	35.69	30.0×5	20.3 ± 0.18
Jun 12.357	P60	i'	35.71	30.0×5	>20.3
Jun 12.358	P60	i'	35.72	30.0×5	>20.3
Jun 12.358	P60	i'	35.73	30.0×3	20.3 ± 0.17
Jun 12.358	P60	i'	35.73	30.0×5	20.3 ± 0.17
Jun 12.359	P60	i'	35.75	30.0×3	20.2 ± 0.18
Jun 12.360	P60	i'	35.78	30.0×5	20.2 ± 0.18
Jun 12.361	P60	i'	35.79	30.0×5	20.3 ± 0.18
Jun 12.361	P60	i'	35.80	30.0×5	>20.4
Jun 12.362	P60	i'	35.82	30.0×5	20.3 ± 0.18
Jun 12.362	P60	i'	35.83	30.0×3	20.3 ± 0.20
Jun 12.362	P60	i'	35.83	30.0×5	20.1 ± 0.18
Jun 12.363	P60	i'	35.85	30.0×3	20.1 ± 0.18
Jun 12.364	P60	i'	35.86	30.0×3	20.0 ± 0.17
Jun 12.364	P60	i'	35.87	30.0×3	20.2 ± 0.18
Jun 12.365	P60	i'	35.89	30.0×3	>20.4
Jun 12.365	P60	i'	35.90	30.0×3	20.2 ± 0.17
Jun 12.367	P60	i'	35.93	30.0×1	>20.4
Jun 12.367	P60	i'	35.93	30.0×3	19.9 ± 0.16
Jun 12.367	P60	i'	35.95	30.0×1	20.0 ± 0.16
Jun 12.368	P60	i'	35.96	30.0×1	20.2 ± 0.19
Jun 12.369	P60	i'	35.99	30.0×3	20.3 ± 0.18
Jun 12.370	P60	i'	36.00	30.0×3	20.2 ± 0.16
Jun 12.370	P60	i'	36.02	30.0×3	20.0 ± 0.16
Jun 12.371	P60	i'	36.03	30.0×3	20.0 ± 0.16
Jun 12.371	P60	i'	36.04	30.0×1	>20.4
Jun 12.371	P60	i'	36.04	30.0×3	>20.4
Jun 12.372	P60	i'	36.07	30.0×3	20.2 ± 0.19
Jun 12.373	P60	i'	36.09	30.0×3	20.2 ± 0.17
Jun 12.374	P60	i'	36.10	30.0×3	>20.4
Jun 12.374	P60	i'	36.11	30.0×3	20.3 ± 0.17
Jun 12.375	P60	i'	36.13	30.0×1	>20.4
Jun 12.375	P60	i'	36.13	30.0×3	20.2 ± 0.18
Jun 12.376	P60	i'	36.16	30.0×3	20.3 ± 0.18
Jun 12.377	P60	i'	36.18	30.0×5	20.3 ± 0.17
Jun 12.378	P60	i'	36.20	30.0×1	>20.4

TABLE 5 — Continued

Epoch (2007 UT)	Facility	Filter	Time Since Burst (hr)	Exposure (s)	Magnitude
Jun 12.378	P60	i'	36.20	30.0×5	>20.4
Jun 12.378	P60	i'	36.21	30.0×1	16.7 ± 0.12
Jun 12.379	P60	i'	36.23	30.0×1	19.2 ± 0.12
Jun 12.379	P60	i'	36.24	30.0×1	19.0 ± 0.13
Jun 12.380	P60	i'	36.26	30.0×1	>20.4
Jun 12.381	P60	i'	36.28	30.0×3	20.0 ± 0.16
Jun 12.381	P60	i'	36.28	30.0×5	20.4 ± 0.17
Jun 12.382	P60	i'	36.30	30.0×3	20.3 ± 0.18
Jun 12.382	P60	i'	36.31	30.0×3	20.3 ± 0.18
Jun 12.384	P60	i'	36.34	30.0×1	>20.4
Jun 12.384	P60	i'	36.34	30.0×3	>20.4
Jun 12.384	P60	i'	36.34	30.0×5	20.3 ± 0.18
Jun 12.384	P60	i'	36.35	30.0×1	18.5 ± 0.13
Jun 12.385	P60	i'	36.37	30.0×1	19.9 ± 0.16
Jun 12.385	P60	i'	36.38	30.0×1	>20.5
Jun 12.386	P60	i'	36.41	30.0×3	20.0 ± 0.17
Jun 12.387	P60	i'	36.42	30.0×3	20.1 ± 0.17
Jun 12.388	P60	i'	36.44	30.0×1	>20.5
Jun 12.388	P60	i'	36.44	30.0×3	20.2 ± 0.19
Jun 12.388	P60	i'	36.45	30.0×1	17.5 ± 0.11
Jun 12.389	P60	i'	36.47	30.0×1	19.3 ± 0.14
Jun 12.389	P60	i'	36.48	30.0×1	>20.4
Jun 12.391	P60	i'	36.52	30.0×5	20.3 ± 0.17
Jun 12.392	P60	i'	36.54	30.0×3	20.3 ± 0.18
Jun 12.392	P60	i'	36.54	30.0×5	20.3 ± 0.17
Jun 12.393	P60	i'	36.57	30.0×5	20.4 ± 0.18
Jun 12.394	P60	i'	36.58	30.0×5	20.4 ± 0.19
Jun 12.394	P60	i'	36.59	30.0×1	>20.4
Jun 12.394	P60	i'	36.59	30.0×5	20.4 ± 0.19
Jun 12.395	P60	i'	36.61	30.0×1	19.6 ± 0.15
Jun 12.395	P60	i'	36.62	30.0×1	20.0 ± 0.15
Jun 12.397	P60	i'	36.65	30.0×3	20.3 ± 0.19
Jun 12.397	P60	i'	36.65	30.0×5	20.4 ± 0.19
Jun 12.397	P60	i'	36.67	30.0×3	20.3 ± 0.19
Jun 12.398	P60	i'	36.68	30.0×1	>20.4
Jun 12.398	P60	i'	36.68	30.0×3	20.4 ± 0.18
Jun 12.398	P60	i'	36.69	30.0×1	18.7 ± 0.13
Jun 12.399	P60	i'	36.71	30.0×1	>20.5
Jun 12.400	P60	i'	36.74	30.0×3	20.2 ± 0.18
Jun 12.401	P60	i'	36.75	30.0×3	20.3 ± 0.19
Jun 12.401	P60	i'	36.76	30.0×3	20.4 ± 0.18
Jun 12.402	P60	i'	36.79	30.0×5	20.5 ± 0.19
Jun 12.403	P60	i'	36.81	30.0×5	20.4 ± 0.19
Jun 12.404	P60	i'	36.82	30.0×3	20.3 ± 0.18
Jun 12.404	P60	i'	36.82	30.0×5	20.3 ± 0.18
Jun 12.404	P60	i'	36.84	30.0×3	20.1 ± 0.18
Jun 12.405	P60	i'	36.85	30.0×1	>20.5
Jun 12.405	P60	i'	36.85	30.0×3	>20.5
Jun 12.405	P60	i'	36.86	30.0×1	>20.6
Jun 12.406	P60	i'	36.88	30.0×1	>20.6
Jun 12.407	P60	i'	36.89	30.0×1	>20.6
Jun 12.407	P60	i'	36.91	30.0×1	>20.6
Jun 12.408	P60	i'	36.92	30.0×1	>20.6
Jun 12.408	P60	i'	36.93	30.0×1	>20.7
Jun 12.409	P60	i'	36.95	30.0×1	>20.7
Jun 12.411	P60	i'	37.01	30.0×5	20.5 ± 0.18
Jun 12.412	P60	i'	37.02	30.0×5	20.5 ± 0.18
Jun 12.413	P60	i'	37.03	30.0×5	20.7 ± 0.20
Jun 12.413	P60	i'	37.05	30.0×3	20.5 ± 0.17
Jun 12.413	P60	i'	37.05	30.0×5	20.7 ± 0.20
Jun 12.414	P60	i'	37.06	30.0×3	20.6 ± 0.19
Jun 12.415	P60	i'	37.09	30.0×5	20.5 ± 0.19
Jun 12.415	P60	i'	37.11	30.0×5	>20.7
Jun 12.416	P60	i'	37.12	30.0×3	20.6 ± 0.20
Jun 12.416	P60	i'	37.12	30.0×5	20.7 ± 0.21
Jun 12.417	P60	i'	37.13	30.0×1	>20.7
Jun 12.417	P60	i'	37.13	30.0×3	20.5 ± 0.18
Jun 12.417	P60	i'	37.15	30.0×1	>20.7
Jun 12.418	P60	i'	37.16	30.0×1	>20.7
Jun 12.419	P60	i'	37.19	30.0×1	>20.6
Jun 12.419	P60	i'	37.19	30.0×3	20.6 ± 0.19
Jun 12.420	P60	i'	37.21	30.0×1	19.6 ± 0.15
Jun 12.420	P60	i'	37.22	30.0×1	20.4 ± 0.20

TABLE 5 — Continued

Epoch (2007 UT)	Facility	Filter	Time Since Burst (hr)	Exposure (s)	Magnitude
Jun 12.421	P60	i'	37.25	30.0×1	20.0 ± 0.19
Jun 12.421	P60	i'	37.25	30.0×3	20.0 ± 0.17
Jun 12.422	P60	i'	37.26	30.0×1	19.3 ± 0.14
Jun 12.423	P60	i'	37.28	30.0×1	20.4 ± 0.18
Jun 12.424	P60	i'	37.31	30.0×3	20.5 ± 0.18
Jun 12.424	P60	i'	37.32	30.0×3	>20.7
Jun 12.425	P60	i'	37.33	30.0×1	>20.6
Jun 12.425	P60	i'	37.33	30.0×3	20.6 ± 0.21
Jun 12.426	P60	i'	37.35	30.0×1	>20.6
Jun 12.426	P60	i'	37.36	30.0×1	>20.6
Jun 12.427	P60	i'	37.38	30.0×1	>20.6
Jun 12.427	P60	i'	37.39	30.0×1	19.6 ± 0.15
Jun 12.428	P60	i'	37.41	30.0×1	>20.6
Jun 12.429	P60	i'	37.42	30.0×1	>20.6
Jun 12.429	P60	i'	37.44	30.0×1	19.7 ± 0.14
Jun 12.430	P60	i'	37.45	30.0×1	19.8 ± 0.16
Jun 12.430	P60	i'	37.46	30.0×1	>20.6
Jun 12.432	P60	i'	37.49	30.0×3	20.4 ± 0.19
Jun 12.432	P60	i'	37.51	30.0×1	>20.5
Jun 12.432	P60	i'	37.51	30.0×3	>20.6
Jun 12.433	P60	i'	37.52	30.0×1	19.6 ± 0.13
Jun 12.433	P60	i'	37.54	30.0×1	19.8 ± 0.14
Jun 12.434	P60	i'	37.55	30.0×1	>20.5
Jun 12.435	P60	i'	37.58	30.0×3	20.4 ± 0.19
Jun 12.436	P60	i'	37.59	30.0×3	20.6 ± 0.20
Jun 12.436	P60	i'	37.61	30.0×1	>20.6
Jun 12.436	P60	i'	37.61	30.0×3	20.5 ± 0.19
Jun 12.437	P60	i'	37.62	30.0×1	18.5 ± 0.13
Jun 12.454	P60	i'	38.02	30.0×1	20.1 ± 0.18
Jun 12.455	P60	i'	38.05	30.0×3	20.4 ± 0.18
Jun 12.455	P60	i'	38.06	30.0×3	20.4 ± 0.18
Jun 12.456	P60	i'	38.08	30.0×1	20.2 ± 0.19
Jun 12.456	P60	i'	38.08	30.0×3	20.2 ± 0.17
Jun 12.457	P60	i'	38.09	30.0×1	19.9 ± 0.18
Jun 12.457	P60	i'	38.10	30.0×1	20.4 ± 0.18
Jun 12.458	P60	i'	38.12	30.0×1	20.1 ± 0.20
Jun 12.458	P60	i'	38.13	30.0×1	>20.4
Jun 12.459	P60	i'	38.15	30.0×1	19.9 ± 0.17
Jun 12.460	P60	i'	38.16	30.0×1	19.6 ± 0.15
Jun 12.460	P60	i'	38.18	30.0×1	>20.4
Jun 12.461	P60	i'	38.21	30.0×3	20.0 ± 0.17
Jun 12.462	P60	i'	38.22	30.0×3	20.2 ± 0.17
Jun 12.463	P60	i'	38.24	30.0×3	20.4 ± 0.18
Jun 12.463	P60	i'	38.25	30.0×3	20.2 ± 0.16
Jun 12.464	P60	i'	38.26	30.0×1	>20.4
Jun 12.464	P60	i'	38.26	30.0×3	20.0 ± 0.15
Jun 12.464	P60	i'	38.28	30.0×1	20.4 ± 0.20
Jun 12.465	P60	i'	38.29	30.0×1	19.0 ± 0.13
Jun 12.466	P60	i'	38.31	30.0×1	20.1 ± 0.16
Jun 12.466	P60	i'	38.32	30.0×1	20.3 ± 0.18
Jun 12.467	P60	i'	38.35	30.0×3	20.1 ± 0.17
Jun 12.468	P60	i'	38.37	30.0×3	20.2 ± 0.18
Jun 12.469	P60	i'	38.38	30.0×1	>20.4
Jun 12.469	P60	i'	38.38	30.0×3	20.1 ± 0.17
Jun 12.470	P60	i'	38.41	30.0×3	20.0 ± 0.16
Jun 12.470	P60	i'	38.43	30.0×3	20.0 ± 0.17
Jun 12.471	P60	i'	38.44	30.0×3	>20.4
Jun 12.472	P60	i'	38.45	30.0×3	20.2 ± 0.18
Jun 12.472	P60	i'	38.47	30.0×3	20.0 ± 0.15
Jun 12.473	P60	i'	38.48	30.0×3	20.0 ± 0.15
Jun 12.473	P60	i'	38.50	30.0×3	20.1 ± 0.16
Jun 12.474	P60	i'	38.52	30.0×3	20.2 ± 0.17
Jun 12.475	P60	i'	38.53	30.0×3	20.2 ± 0.18
Jun 12.476	P60	i'	38.56	30.0×5	20.1 ± 0.18
Jun 12.477	P60	i'	38.58	30.0×5	20.2 ± 0.18
Jun 12.477	P60	i'	38.59	30.0×3	20.1 ± 0.17
Jun 12.477	P60	i'	38.59	30.0×5	20.2 ± 0.17
Jun 12.478	P60	i'	38.61	30.0×3	20.1 ± 0.17
Jun 12.479	P60	i'	38.62	30.0×3	19.7 ± 0.15
Jun 12.479	P60	i'	38.63	30.0×1	>20.0
Jun 12.479	P60	i'	38.63	30.0×3	>20.1
Jun 12.481	P60	i'	38.68	30.0×5	>19.8
Jun 12.482	P60	i'	38.70	30.0×1	19.4 ± 0.15

TABLE 5 — Continued

Epoch (2007 UT)	Facility	Filter	Time Since Burst (hr)	Exposure (s)	Magnitude
Jun 12.482	P60	i'	38.70	30.0×5	19.7 ± 0.16
Jun 13.239	P60	i'	56.86	60.0×137	>20.2
Jun 14.413	P60	i'	85.05	$180. \times 6$	>18.4
Jun 15.232	P60	i'	104.7	$180. \times 6$	>18.3
Jun 16.407	P60	i'	132.9	$180. \times 12$	>18.8
Jun 17.227	P60	i'	152.5	$180. \times 6$	>18.3
Jun 18.380	P60	i'	180.2	$180. \times 6$	>18.4
Jun 19.344	P60	i'	203.3	$180. \times 6$	>18.5
Jun 20.370	P60	i'	228.0	$180. \times 6$	>18.4

NOTE. — Error quoted are 1σ photometric and instrumental errors summed in quadrature. Note that the uncertainty in the zeropoint estimate (relative to USNO-B stars) dominates but is an overestimate for variability studies using relative magnitude. Upper limits quote are 3σ . No correction has been made for the large (and uncertain) line-of-sight extinction.